Bioactive Materials 33 (2024) 129–156

Contents lists available at ScienceDirect

Bioactive Materials

journal homepage: www.keaipublishing.com/en/journals/bioactive-materials

Review article

Biomaterial scaffolds in maxillofacial bone tissue engineering: A review of recent advances

Xiangya Huang [a,b,1], Yaxin Lou [a,b,1], Yihong Duan [a,b], He Liu [c], Jun Tian [a,b], Ya Shen [c,*], Xi Wei [a,b,**]

[a] Hospital of Stomatology, Guanghua School of Stomatology, Sun Yat-Sen University, Guangzhou, China
[b] Guangdong Provincial Key Laboratory of Stomatology, Guangzhou, China
[c] Division of Endodontics, Department of Oral Biological and Medical Sciences, The University of British Columbia, Vancouver, British Columbia, Canada

ARTICLE INFO

Keywords:
Biomaterial scaffolds
Maxillofacial region
Bone regeneration
Tissue engineering

ABSTRACT

Maxillofacial bone defects caused by congenital malformations, trauma, tumors, and inflammation can severely affect functions and aesthetics of maxillofacial region. Despite certain successful clinical applications of biomaterial scaffolds, ideal bone regeneration remains a challenge in maxillofacial region due to its irregular shape, complex structure, and unique biological functions. Scaffolds that address multiple needs of maxillofacial bone regeneration are under development to optimize bone regeneration capacity, costs, operational convenience. etc. In this review, we first highlight the special considerations of bone regeneration in maxillofacial region and provide an overview of the biomaterial scaffolds for maxillofacial bone regeneration under clinical examination and their efficacy, which provide basis and directions for future scaffold design. Latest advances of these scaffolds are then discussed, as well as future perspectives and challenges. Deepening our understanding of these scaffolds will help foster better innovations to improve the outcome of maxillofacial bone tissue engineering.

1. Introduction

Maxillofacial bone defects can be caused by congenital malformations, trauma, tumors, and inflammation. These defects severely affect the function and aesthetics of the jaw, leading to a reduction in the patient's quality of life. However, regenerating bone in the maxillofacial region is clinically challenging due to the area's irregular shape, complex structure, and biological functions.

Successful bone repair requires the interplay of stem cells and numerous growth factors within the healing niche. When large bone defects exceed the "critical size," natural healing is hopeless, and measures like bone grafts or substitutes implantation should be taken [1]. Autografts have been considered the "gold standard" for bone repair for over a century [2]. However, recent studies have shown that alveolar bone tissue engineering using α-tricalcium phosphate loaded with or without mesenchymal stem cells (MSCs) is equally effective, raising questions about whether autografts are still the gold standard for the repair of alveolar bone defects [3].

Tissue engineering and regenerative medicine have drawn great attention in recent decades, and a variety of studies are underway to evaluate biomaterial-based strategies for better regeneration of maxillofacial bone. Biomaterial scaffolds provide support for cell growth, deliver cell signals, and exert dramatic influences on the microenvironment of tissue formation. Different types of biomaterials, such as bone grafts, bioceramics, natural and synthetic polymers, and tooth derivates, have been applied clinically in the maxillofacial region. However, there are still drawbacks like unsatisfying amounts and structures of regenerated bone, complications, or a lack of long-term stability [4]. Therefore, it is crucial to refine our understanding of the requisites and status quo of maxillofacial bone tissue engineering to

Peer review under responsibility of KeAi Communications Co., Ltd.
* Corresponding author. Division of Endodontics, Department of Oral Biological & Medical Sciences, Faculty of Dentistry, The University of British Columbia, Vancouver, BC, V6T 1Z3, Canada.
** Corresponding author. Hospital of Stomatology, Guanghua School of Stomatology, Sun Yat-Sen University, 56 Ling Yuan Xi Road, Guangzhou, 510055, China.
E-mail addresses: hxiangya@mail.sysu.edu.cn (X. Huang), louyx5@mail2.sysu.edu.cn (Y. Lou), duanyihong526@gmail.com (Y. Duan), he.liu@ubc.ca (H. Liu), tianjun2@mail2.sysu.edu.cn (J. Tian), yashen@dentistry.ubc.ca (Y. Shen), weixi@mail.sysu.edu.cn (X. Wei).
[1] Xiangya Huang and Yaxin Lou contributed equally to this work.

https://doi.org/10.1016/j.bioactmat.2023.10.031
Received 28 August 2023; Received in revised form 30 October 2023; Accepted 30 October 2023

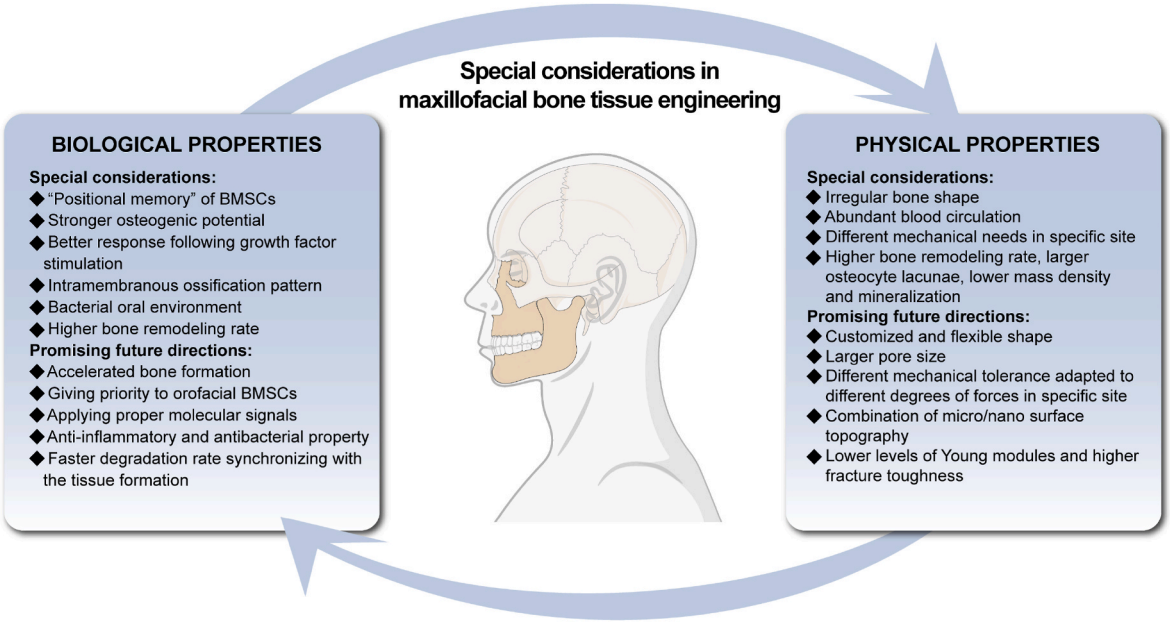

Fig. 1. Special considerations in scaffold design for bone tissue engineering in maxillofacial regions.

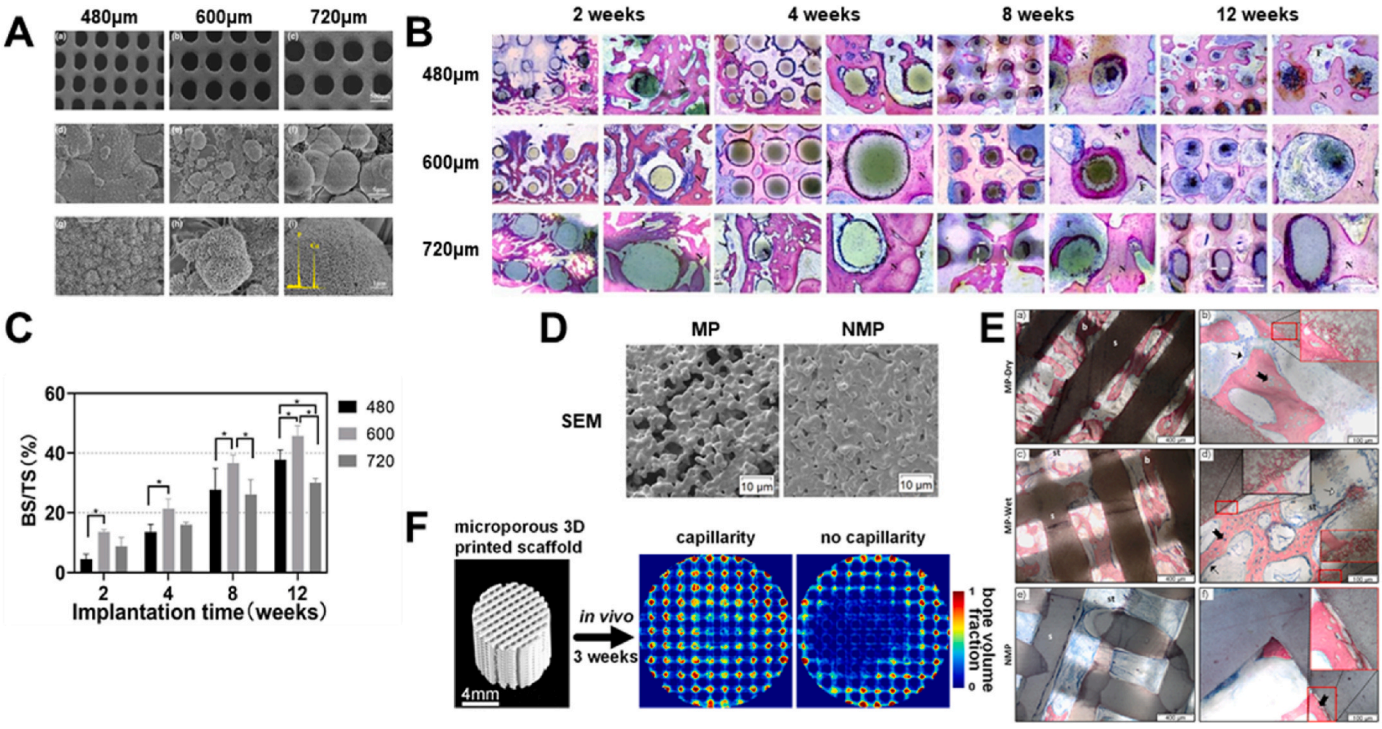

Fig. 2. Macropore (>100 μm) size and controlled microporosity (<20 μm) can significantly influence bone regeneration. (A) Scanning electron micrographs (SEM) showed surface texture (a–c) and remineralization of scaffolds (d–i) with different pore size (480, 600, and 720 μm) after soaking in simulated body fluid liquid for 14 days. The formation of hydroxyapatite clusters became larger as the pore size increased (d–i), with a Ca/P ratio of 1.57(i). (B–C) McNeal staining (40 × , 100 ×) (B) and quantitative analysis (C) of bone regeneration were shown in rabbit mandibular defect model. Reprinted with permission from Ref. [13]. (D) Rod structure of the microporous (MP) or non-microporous (NMP) biphasic calcium phosphate (BCP) scaffold. (E) Histological evaluation of MP or NMP scaffolds in pig mandibular defect model. In the macropores of MP scaffolds, mineralized bone is anchored in rods (b and d). In NMP, bone is not anchored (f). (b, new bone; s, scaffold rods; st, fibrous soft tissue.) (F) Photograph illustration of microporous 3D printed scaffold and the effect of capillarity on in vivo bone formation. Reprinted with permission from Ref. [17].

develop more ideal biomaterial scaffolds for maxillofacial bone regeneration that will fully recover the normal physiologic functions of the defect areas.

This article highlights the special considerations for bone tissue engineering in maxillofacial regions, elaborates on a series of current clinical explorations for maxillofacial bone repair, and summarizes the latest advances in maxillofacial bone tissue engineering. Potential challenges of future research and obstacles in clinical translation are also discussed.

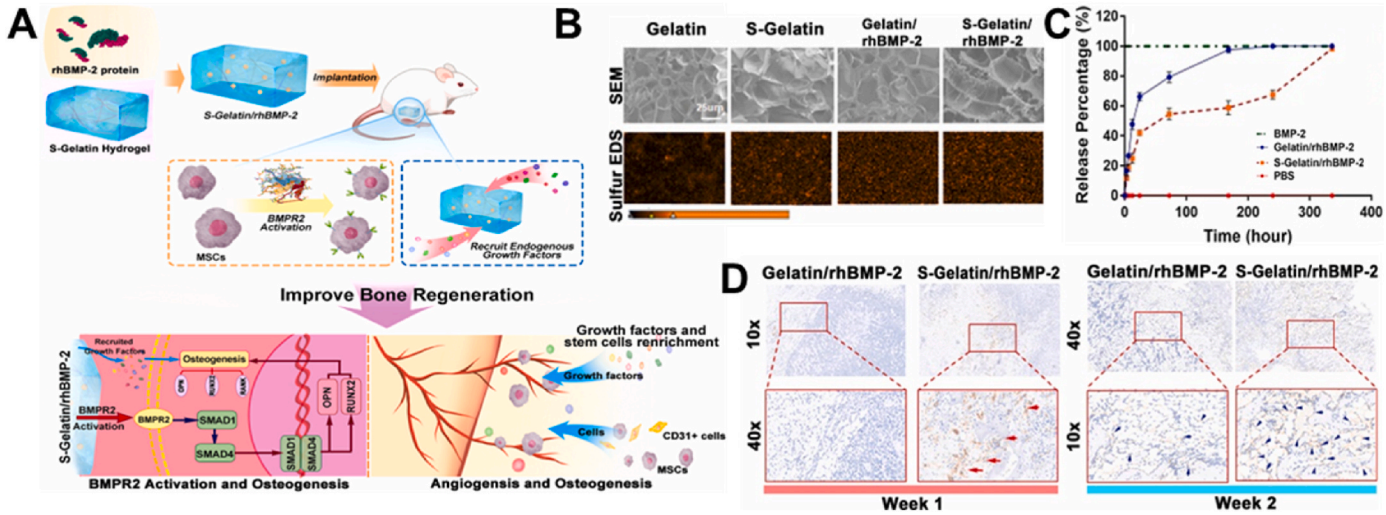

Fig. 3. S-Gelatin/recombinant human BMP-2 (rhBMP-2) hydrogel could enhance angiogenesis and osteogenesis. (A) S-Gelatin/rhBMP-2 hydrogel could rapidly activate BMP-2 type II receptors (BMPR2) on MSCs to induce differentiation and cytokine secretion to recapitulate in situ osteogenesis. (B) The SEM and energy spectrum analysis (EDS) of hydrogels. (C) The release behavior of rhBMP-2 in the hydrogels. (D) CD31 staining was evidently increased in S-Gelatin/rhBMP-2 compared with that in Gelatin/rhBMP-2 in vivo. Reprinted with permission from Ref. [39].

Table 1
Clinical trials on alveolar bone augmentation with different biomaterials.

Subject number (age)	Intervention	Follow-up	Outcome	Severe complications	Ref.
11 (49.91 ± 12.95)	Decellularized, degreased cancellous bovine bone	8 m post-surgery 12 m post loading	Bone height increased by 1.95 ± 0.19 mm, 2.39 ± 0.38 mm, 2.91 ± 0.56 mm, 3.28 ± 0.63 mm at 12 months post loading at four measured planes.	——	[52]
15 (54.5 ± 8.34)	Collagenated xenogeneic bone block (Bio-Graft®)	24w	84.6 % attained enough bone volume for implant insertion without additional contouring.	33.3 % soft tissue dehiscence, 1 case of allergy.	[49]
5 (mean 51.6)	Bio-Graft®	Mean 28.9 month	Horizontal width gain of 3.6 ± 1.22 mm.	Graft failure in 4 of 5 patients, Averagely 67.3 ± 9.5 % of soft connective tissue within grafts.	[50]
40 (control: 50.85 ± 7.71; test: 49.05 ± 7.76)	Control: Bio-Oss® Test: PRF + Bio-Oss®	6 m post-surgery 2y post-loading	Mean augmentation thickness: test (1.63 ± 0.21 mm, 2.59 ± 0.34 mm, 3.11 ± 0.36 mm at all measured levels) > control (1.34 ± 0.14 mm, 2.49 ± 0.24 mm, and 2.97 ± 0.24 mm)	——	[53]
18 (mean 56.8)	1:1 mixture of Bio-Oss® + autologous bone (AB)	7 m post-surgery 3y post-loading	Average horizontal bone gain of 5.03 ± 2.15 mm	——	[54]
38 (45 ± 13)	AB	10y	Implant success rate of 98.1 % and graft resorption of 7.7 % after 10 years. Gender (more resorbed in females) and donor site (chin > retromolar) affect resorption.	–	[51]
28 (mean 65.8)	Corticocancellous or cancellous freeze-dried bone allograft (FDBA)	4 m post-grafting, 24 m post-implant placement	Implant survival rate of 100 % Resorption rate: cancellous grafts (29.2 % ± 2.6) > corticocancellous grafts (19.3 % ± 2.3). Grafts in recipients with low bone density and smokers are resorbed more prominently.	——	[55]
40 (not specified)	Control: FDBA Test: FDBA + AB	6 m	Similar augmentation outcomes.	–	[56]
30 (48.5 ± 17)	Control: FDBA; Test: thick and expandable multilayer sugar cross-linked collagen scaffold (Ossix Volumax, OV).	9 m	Sites volume increase: control (from 266 ± 149 mm^3 to 360 ± 138 mm^3) > test (negligible).	–	[58]

2. Optimizing scaffold design for bone tissue engineering in maxillofacial regions: special considerations (Fig. 1)

2.1. Considerations in physical properties

2.1.1. Customized shape

The contour and continuity of maxillofacial bone play a crucial role in both facial symmetry and oral function. Scaffold architecture largely determines the shape of newly formed bone [5], making it essential for the scaffold to fit the irregular shape of maxillofacial bone. To achieve this, three-dimensional (3D) printing combined with computer digital technology has emerged as a promising technique for scaffold manufacture due to its precise control over the fabrication process and ease of use. The resulting 3D-printed macro-microstructures can mimic the desired tissue morphology and serve as excellent delivery vehicles for local, sustained release of drugs and/or biomolecules [6]. In addition to solid 3D scaffolds, injectable materials, such as shape-adaptable in-situ gelatinizing hydrogel scaffolds, have also been developed to fill irregular bone defects with undercuts. For example, Zhou et al. created a biomimetic porous hydrogel with controllable magnesium ion release for accelerated bone regeneration, which undergoes a liquid-to-solid phase transition when injected into bone defects [7]. Thermal-sensitive

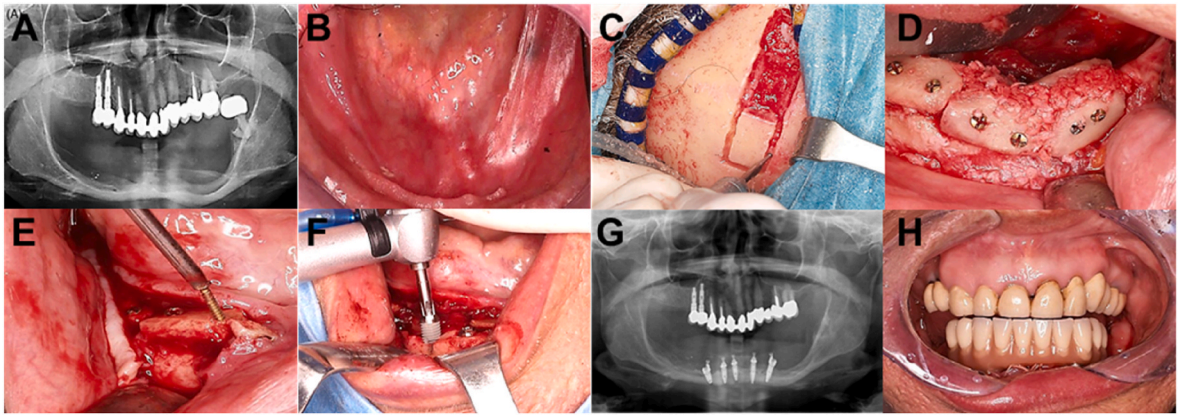

Fig. 4. Application of biomaterial scaffolds in alveolar bone regeneration. (A–B) Preoperative radiographical and clinical view of a patient with severe ridge resorption. (C–D) Harvest calvarial bone at donor site and fix the grafts in the mandibular recipient site. (E–F) After graft integration, osteosynthesis screws were removed and dental implants were placed. (G–H) Radiographical and clinical view after implant prosthetic rehabilitation. Reprinted with permission from Ref. [57].

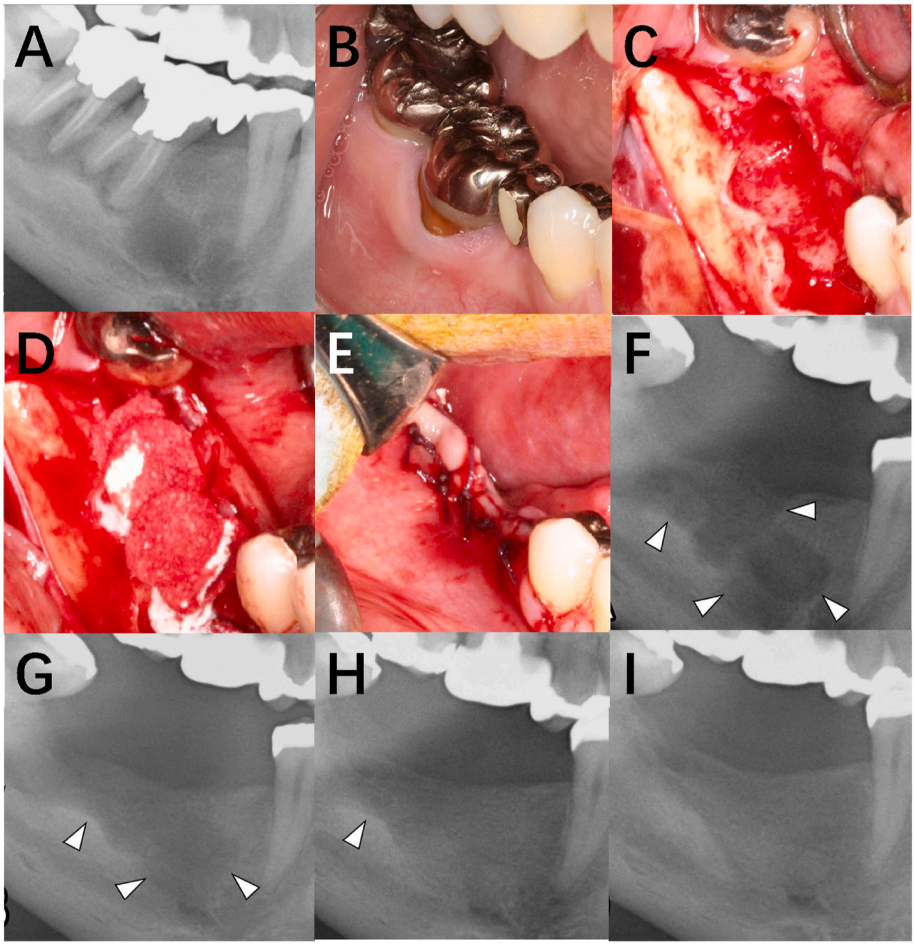

Fig. 5. Application of biomaterial scaffolds in jawbone defect repair. (A) Pre-operative radiograph shows a radiolucent area of the right mandible in a 42-year-old Japanese male. (B) Intraoral photograph of the right mandibular region. (C) Large jawbone defect was detected after cystectomy and extraction of the first and second molars. (D–E) The defect area was implanted with octacalcium phosphate–collagen sponge disks and sutured. (F–I) Radiographs on the day after the operation and after 3, 6, and 12 postoperative months show the repair of jawbone. Reprinted with permission from Ref. [61].

hydrogels with excellent in-situ injectability and controlled biomolecule delivery have also shown promise in enhancing bone regeneration in critical-sized calvarial bone defects or periodontal tissues [8,9]. However, controlling the flow of hydrogel during injection to a specific site can sometimes be difficult due to gravity. Thus, combining 3D scaffolds with hydrogels may offer a possible strategy to overcome this challenge.

2.1.2. *Pore geometry*

The design of bone tissue engineering scaffolds should prioritize creating a three-dimensional and highly porous space with an interconnected pore network to support cell growth. The scaffold's pore interconnectivity is directly linked to vascularization, cell seeding, guided cell migration, transportation of nutrients and metabolic waste,

Table 2
Clinical studies using biomaterials for jawbone defects.

Patient number (age)	Disease/condition	Intervention	Follow-up	Outcome	Severe complications	Ref.
54 (range 10–65)	Large mandibular defect due to benign tumors	Non-vascularized iliac bone graft	3y	The complete survival rate of grafts was 87.0 %, and the partial survival rate was 98.1 % (6 cases of chronic fistulas were included).	2 cases of submandibular effusion, 2 submandibular abscesses, 6 chronic oral fistulas, 1 graft failure.	[59]
8 (mean 36)	Complex zygomatico-maxillary defects	3D-printed polycaprolactone/ beta tricalcium phosphate (PCL/ β-TCP) scaffold	6 m	Mean bone fraction volume (newly formed bone/total implant volume) of 23.34 % (range 7.81%–66.21 %).	1 case of implant exposure in a patient who had undergone radiation treatment, possible allergy.	[60]

Table 3
Clinical studies using biomaterials for periapical defects.

Patient number (age)	condition/disease	Intervention	Follow-up	Outcome	Ref.
33 (not specified)	apical surgery	Control Test1: MTA Test2: PRF Test3: MTA + PRF	1y	Lesion volume reduction: test1≈test3 > test2≈control.	[62]
44 (mean control: 49.7; test1: 44.8; test2: 44.9; test3: 43.5)	apical surgery	Control Test1: Bio-Gide® Test2: L-PRF Test3: L-PRF + Bio-Gide®	1y	Lesion volume reduction: test1 ≈ test3 > test2 ≈ control.	[63]
20 (mean 24)	apical surgery	Control Test: PRP + calcium sulfate (CS) + AB	20w	The mean percentage increase in bone formation: test (87 %) > control (49 %).	[64]
32 (27.84 ± 5.5)	through-and -through apical lesion	Control Test: PRP	1y	Success rate: test (87.5 %) > control (50 %). Lesion volume reduction: test (92.30 % ± 4.72 %) > control (83.04 % ± 12.82 %).	[66]
30(control: 25.67 ± 6.83; test: 27.93 ± 8.30)	apicomarginal defects of endodontic origin	Control Test: PRF	1y	Similar success rates.	[65]

and tissue ingrowth, all of which are critical for osteogenesis during the first 4 weeks after implantation [10,11].

Pore size is another essential factor influencing bone tissue ingrowth, bearing strength, and soft tissue invasion. The optimal pore size range for bone regeneration scaffolds is typically considered to be 300–500 μm, with porosity in the 70–90 % range, promoting bone ingrowth, vascularization, and innervation [12]. However, a recent study has proposed a new ideal pore/bottleneck dimension of 700-1200 μm, which is two to four-fold larger than previously believed [11]. In the maxillofacial region, where abundant blood circulation is required, adjusting the pore dimension to 600 μm may be the most beneficial for repairing mandibular bone defects compared with 480 and 720 μm, as demonstrated in a rabbit mandibular defect model (Fig. 2A–C) [13]. A possible explanation is that large pore size facilitates the nutrient and oxygen supply and thus enhances osteogenesis. However, the nutrient and oxygen supply will be saturated when pore dimension is increased to a particular size, and the large pore dimension is not conducive to bone interconnectivity. Additionally, pore size needs to be tailored to different forces in specific surgical sites. A pore size of 750 μm may enhance cell infiltration in areas with lower forces, such as the sinus floor, while a pore size of 490 μm is better suited for load-bearing areas, such as the lateral mandible, to withstand strong forces during mastication [14]. The potential invasion of soft tissue should also be considered in scaffold design, with smaller pore sizes of 200–300 μm preferred for preventing fibrous tissue penetration [15]. When constructing scaffolds with larger pores, it may be necessary to use barrier membranes to achieve superior bone formation. Besides, the uniformity of the pore structure is also critical for tissue engineering, with uniform pore structure within each region and different pore sizes in different regions being a promising solution [16].

2.1.3. Micro-structured topographies

Optimization of macroporous scaffold performance can be achieved through the design of surface micro-structured topographies. Macropores (>100 μm) are critical for bone ingrowth and vascularization, but studies have shown that microporosity (<20 μm) can also enhance bone growth. Controlled microporosity combined with macropores can significantly improve bone regeneration by promoting capillarity and homogeneous bone distribution within the scaffold. When microporous scaffolds were submerged in phosphatic buffered saline (MP-Wet) before implantation and no longer had active micropore-induced capillary forces, homogeneity of bone distribution was impaired (Fig. 2D–F). This approach can be particularly beneficial for treating large and load-bearing bone defects [17]. In addition, the incorporation of different types of micro/nano surface topography in scaffold design has been found to promote osteogenic differentiation of stem cells and enhance bone regeneration by targeting mitogen-activated protein kinase (MAPK), signal transducer and activator of transcription (STAT), and AKT signaling pathways [18]. Micro/nanostructured modifications have also been applied to titania surfaces in implant dentistry to promote bone integration [19]. Physical stimulation of cells by the surface topography of scaffolds can enhance bioactivity and biocompatibility and accelerate bone repair by modulating the physical microenvironment that favors cell and tissue growth at the bone defect site [20].

2.1.4. Mechanical properties

Bone engineering scaffolds should have mechanical properties that match the tissues at the site of implantation to provide adequate mechanical support and prevent excessive deformation, which may lead to failure of nascent tissue formation [21]. Maxillofacial bone has a higher remodeling rate and lower mineralization and mass density compared to femur due to the presence of larger osteocyte lacunae [22,23]. As a result, low values of bone mineralization led to low levels of Young's modulus and high fracture toughness, which should be taken into account when designing scaffolds for maxillofacial bone regeneration [24]. Additionally, bones in different maxillofacial regions exhibit

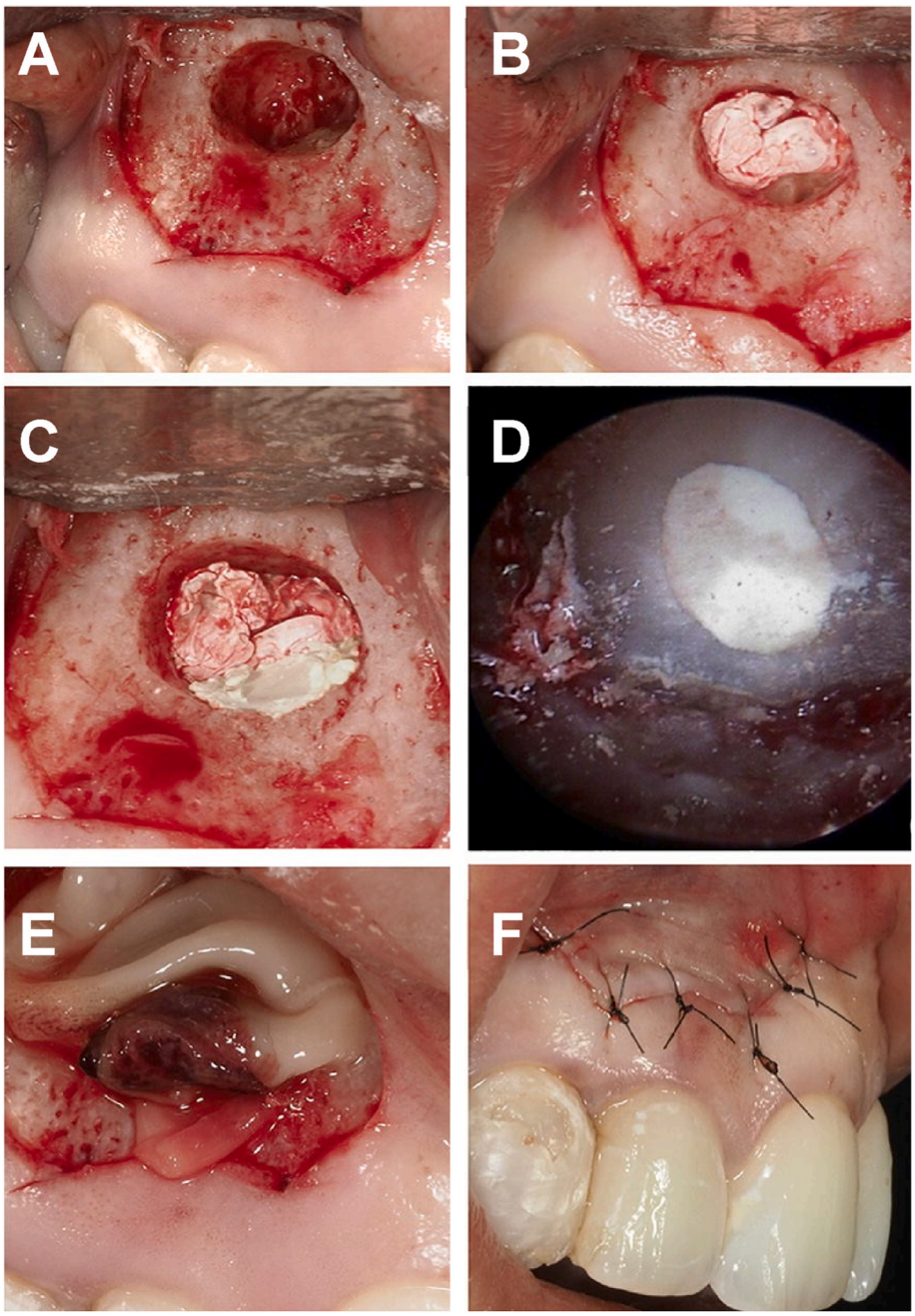

Fig. 6. Application of biomaterial scaffolds in endodontic surgery. (A) Bony crypt after flap elevation and mechanical debridement. (B) Hemostasis with epinephrine-impregnated gauze and PTFE strip. (C) Retrograde obturation with MTA. (D) Root integrity is ascertained by inspection using a rigid endoscope. (E) A-PRF + membrane plied into the bony crypt. (F) Final suturing. Reprinted with permission from Ref. [67].

different mechanical performance. For instance, the trabecular bone in the anterior mandible has a significantly higher density, which leads to higher elastic modulus and ultimate compressive strength compared to other regions [25]. Therefore, scaffold materials and abovementioned pore size should fit mechanical needs of specific sites especially when dealing with large bone defects that involve different maxillofacial regions and need to withstand masticatory forces to fulfill their function. It should be noted that while most experimental studies have characterized the mechanical properties of designed scaffolds and evaluated the quantity and vascularization of newly formed bone tissue, their ability to function effectively under physiological circumstances such as masticatory stress remains to be investigated.

2.2. Considerations in biological properties

2.2.1. Osteogenesis and angiogenesis

Numerous studies have shown that bioengineering of bone tissue involves both osteogenesis of stem cells and angiogenesis [26]. However, the embryonic origin of stem cells may have a considerable impact on bone healing in terms of osteogenesis and angiogenesis, which is often overlooked in practice.

Maxilla and mandible are both derived from neural crest, while long bones are lateral plate mesoderm-derived [27]. The bone marrow mesenchymal stem cells (BMSCs) of different embryonic origins may have site-specific preferences. Leucht et al. reported a “positional memory” of skeletal stem cells, which influences cell behavior when grafted into ectopic locations. For example, neural crest-derived

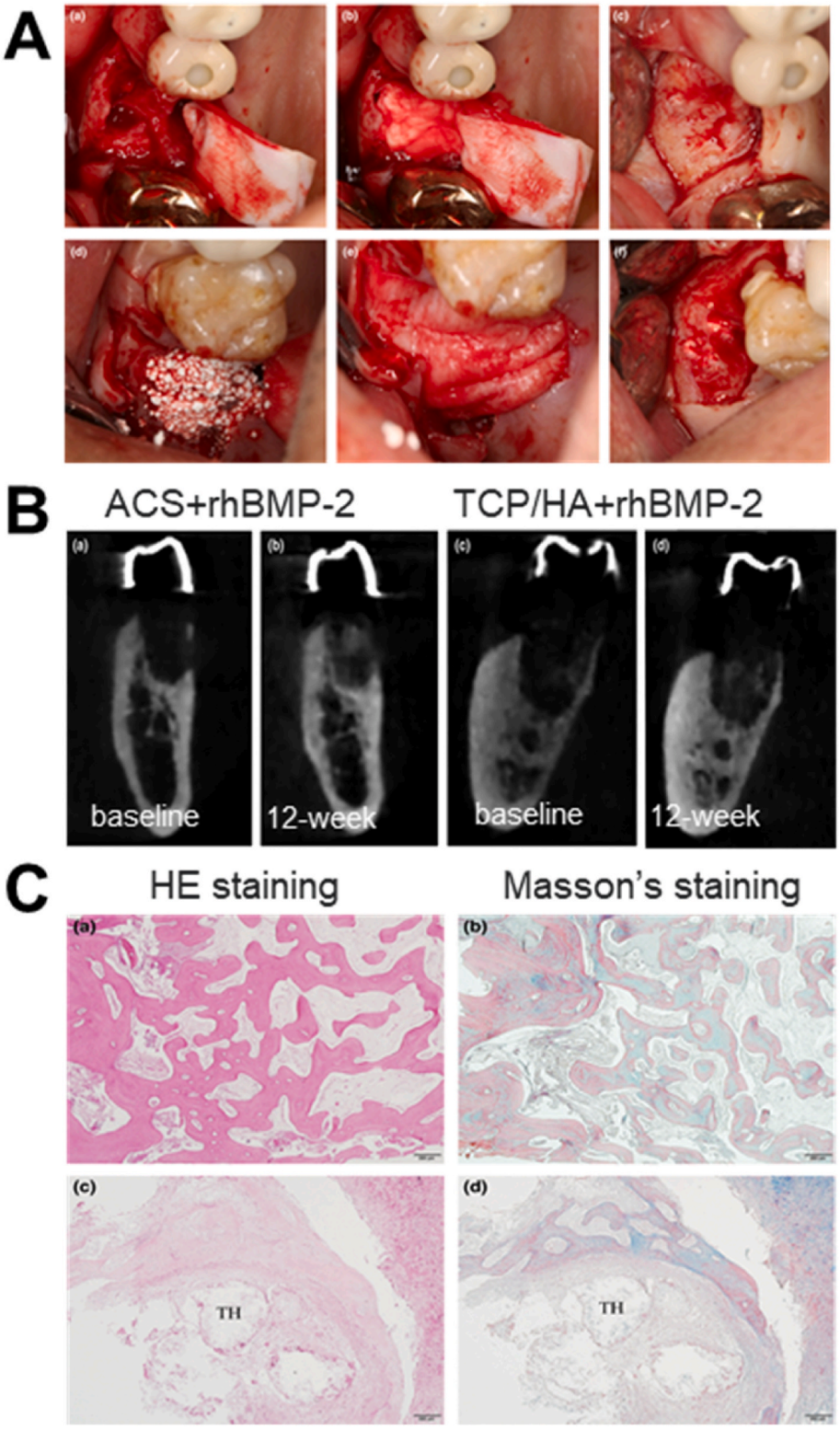

Fig. 7. Application of biomaterial scaffolds in ridge preservation and socket healing. (A) Clinical image of recombinant human bone morphogenetic protein-2 (rhBMP-2) application via loaded absorbable collagen sponge (ACS) (a) and β-tricalcium phosphate and hydroxyapatite (TCP/HA) (d) in tooth extraction socket. The collagen membrane covered the grafted materials (b), (e). Clinical features at 4 months after ridge preservation were shown in (c) and (f). (B) Cross-sectional radiographs at baseline and 12 weeks after ridge preservation. (C) Histological analysis of ridge-preserved sites at 4 months after implantation of ACS + rhBMP-2 (a and b) and TCP/HA + rhBMP-2 (c and d). Reprinted with permission from Ref. [75].

Table 4
Clinical trials on ridge preservation and socket healing with different biomaterials.

Subject number (age)	Disease	Intervention	Follow-up	Outcome	Ref.
24 (44.84 ± 8.62)	Ridge preservation after tooth extraction	Bio-Oss® or FDBA (MinerOss®)	5 m	Similar preservation outcomes.	[76]
39 (control: 51.9 ± 12.1; test: 54.9 ± 8.4)	Ridge preservation after tooth extraction	Control; Test: Bio-Oss Collagen®	6 m	Residual bone height: test (7.30 mm [6.36, 8.20]) > control (4.83 mm [3.94, 5.76]).	[77]
4 (mean 54)	Ridge preservation after tooth extraction	1:1 mixture of autologous particulate dentin + L-PRF, bound with liquid fibrinogen as binder	4–6 m	Successful preservation and even augmentation, dentin particles can be replaced by bone.	[68]
40 (control: 51 ± 14; test1: 48 ± 13; test2: 54 ± 11; test3: 43 ± 19)	Ridge preservation after tooth extraction	Control: natural healing; Test1: autologous plasma rich in growth factor (PRGF); Test2: DBBM; Test3: FDBA	3 m	All test groups significantly reduced alveolar ridge height reduction, and test2 significantly reduced ridge width reduction.	[70]
20 (64.4 ± 12.0)	Ridge preservation after tooth extraction	Control Test1: L-PRF Test2: A-PRF+	3 m	Similar mean ridge width and height changes across the groups. Socket fill: test1 (85.2 %) ≈ test2 (83.8 %) > control (67.9 %).	[72]
40 (mean 58)	Ridge preservation after tooth extraction	Control; Test1: A-PRF; Test2: A-PRF + FDBA; Test3: FDBA	15w	Similar mean ridge width reduction across the groups. Mean ridge height loss: test1(1.8 ± 2.1 mm) and test2 (1.0 ± 2.3 mm) < control (3.8 ± 2.0 mm).	[73]
32 (unspecified)	Ridge preservation after tooth extraction	Group1: PLGA-Coated β-TCP (PLGA-β-TCP) Group2: FDBA particles covered with a rapidly absorbable collagen dressing (RACD)	20w before implant placement and 12 m after prosthesis delivery	Similar preservation of ridge dimensions. Mineralized tissue formation: group2 (38.2 % ± 12.5 %) > group1 (27.0 % ± 22.1 %)	[78]
21 (mean 56.6)	Ridge preservation after tooth extraction	Control: Bio-Oss Collagen® + gingival soft tissue punch Test: Bio-Oss Collagen® + hemostatic gelatin sponge	6 m	Ridge width reduction: test (mean 4.8/2.3/1.3 mm at all measured levels) < control (mean 7.1/4.0/2.5 mm).	[79]
64 (56.00 ± 10.64)	Ridge preservation after tooth extraction	Control: BCP + rhBMP-2 Test:ACS + rhBMP-2	4 m	Similar preservation outcome.	[75]
20 (control: 31.2 ± 6.44; test: 33.5 ± 7.37)	Ridge preservation after tooth extraction	Control: autogenous demineralized dentin graft (ADDG) Test: autogenous whole tooth (AWTG)	6 m	Similar preservation outcome, but control demonstrated better integration.	[69]
42 (52.5 ± 10.8)	Ridge preservation after tooth extraction	Control: Bio-Oss Collagen® Test: Bio-Oss Collagen® + enamel matrix derivative (EMD, Emdogain®)	4 m	New bone formation: test (45.1 ± 8.8 %) > control (16.5 ± 6.9 %). Residual graft: test (20.3 ± 7.2 %) < control (36.8 ± 8.8 %).	[80]
18 (41.67 ± 12.73)	Socket healing	Control; Test: L-PRF	5 m	Similar healing outcomes, despite L-PRF increased the growth factor concentrations in the wound fluid from extraction sockets.	[71]
48 (mean: 44.8)	Socket healing	Control; Test: L-PRF	3 m	Ridge width reduction: test (0.93 ± 0.9 mm) < control (2.27 ± 1.2 mm). New bone formation: test (55.96 ± 11.97 %) > control (39.69 ± 11.13 %).	[74]
48 (range 18–66)	Socket healing	Control B1:HA 60.28 % and β-TCP 39.72 %; B2: HA 78.21 % and β-TCP 21.79 %; Bone Ceramic (BC): HA 61 % and β-TCP 39 %	6 m	New bone formation: B1 (69.3 % ± 6.03 %) > BC (51.6 ± 12.34 %) > B2 (46.6 ± 7.66 %) > control (45.4 ± 7.98 %). B1 formed least connective tissue with least graft residual.	[81]

progenitors tend to repair the mandible, while mesoderm-derived progenitors prefer the tibia. The latter failed to differentiate into osteoblasts for a mandible defect, highlighting the importance of caution when extending results from long bones to maxillofacial bones [28].

BMSCs of different embryonic origins may also exhibit different healing capacities and osteogenic potential. Compared with BMSCs from long bones, orofacial BMSCs demonstrated an increased osteogenic potential and enhanced capacity to induce bone formation. They exhibited more calcium accumulation, quicker proliferation, and delayed senescence in vitro and produced 70 % larger bone nodules containing threefold more mineralized bone in mice [29,30]. BMSCs of alveolar origins transplanted in combination with β-tricalcium phosphate ($Ca_3[PO_4]$, β-TCP) in dog peri-implant bone defects also demonstrated strong osteogenic potential, though no significant difference were found between alveolar and iliac BMSCs [31]. Compared with iliac crest BMSCs, orofacial BMSCs presented better response following growth factor stimulation [32]. This excellent osteogenic ability of orofacial BMSCs would benefit the rate of bone regeneration and supports accelerated bone formation. Therefore, the coordinated degeneration rate of scaffolds should be noted, and orofacial BMSCs should be given priority in the cell-loading strategy of maxillofacial bone regeneration.

It is important to note that the ossification patterns of long bones and maxillofacial bones (except for the condyle) differ, with maxillofacial bones developing via intramembranous ossification rather than endochondral ossification, which is the typical pattern in long bones [33]. Although both patterns begin with mesenchymal condensations, the differentiation of mesenchymal progenitors that follows is distinct, as indicated by the different lineage commitment of either chondroblasts or osteoblasts [34]. This leads to distinct molecular signals following growth factor stimulation for the different modes of bone formation

Table 5
Clinical trials on bone defects in periodontal diseases with different biomaterials.

Subject number (age)	Disease	Intervention	Follow-up	Outcome	Ref.
100 (DBBM group: 54.47 ± 11.00; DPBM group: 56.13 ± 10.20)	Damaged extraction sockets due to periodontal disease	deproteinized bovine bone mineral (DBBM) or porcine bone mineral (DPBM)	4 m	Similar regeneration outcome with minimal postoperative reduction of the grafted volume. But some cases showed large variations in the stability of graft volume.	[88]
29 (50.7 ± 8.5)	3-wall intrabony defects (IBDs) in chronic periodontitis	Control: Collagen sponge scaffold (Condress®); Test: Autologous dental pulp stem cells (DPSC) + Condress®	12 m	Bone defect fill: test (3.9 mm) > control (1.6 mm).	[89]
57 (mean: 39.7)	3-wall IBDs in chronic periodontitis	Control: open-flap debridement (OFD); Test1: PRF + OFD; Test2: PRF + HA + OFD	9 m	Mean bone fill: test2 (63.39 % ± 16.52 %) > test1 (56.46 % ± 9.26 %) > control (15.96 % ± 13.91 %).	[82]
17 (mean: 29.7)	3-wall IBDs in aggressive periodontitis	Control: OFD Test: PRF + OFD	9 m	Bone defect fill: test (46.14 % ± 11.39 %) > control (15.76 % ± 18.77 %).	[83]
20 (control: 28.2 ± 5.63; test: 32 ± 5.27)	2-3 wall IBDs in chronic periodontitis	Control: PRF Test: vitamin C + PRF	6 m	Bone defect fill: test (2.29 ± 0.61 mm) > control (1.63 ± 0.46 mm). Both achieved significant periodontal regeneration.	[90]
30 (control: 43.93 ± 12.85; test: 44.93 ± 13.06)	2-3 wall IBDs	Control Test: EMD + bovine bone substitute	1y	Similar regeneration outcomes, both are significant.	[86]
24 (control: 46.50 ± 10.47; test: 50.33 ± 9.02)	Combined 1-2wall intrabony and supra-bony defects	Control: EMD Test: EMD + bovine bone mineral (Cerabone®)	1y	Similar regeneration outcomes, both are significant.	[87]
24 (mean 35.2)	Grade II Furcation Defect	Control: nanoHA Test: PRF + nanoHA	9 m	Bone defect fill: test (from 2.9 ± 0.88 to 5.6 ± 1.10) > control (from 3.4 ± 1.39 to 3.9 ± 1.4). Both achieved significant periodontal regeneration.	[84]
72 (control: 39.45 ± 5.20; test1: 38.30 ± 5.35; test2: 38.52 ± 5.22)	Grade II Furcation Defect	Control Test1: PRF Test2: PRF + 1 % alendronate gel	9 m	Bone defect fill: test2 (56.01 % ± 2.64 %) > test1 (49.43 % ± 3.70 %) > control (10.25 % ± 3.66 %).	[85]

[35], with differential contributions of various genes encoding either bone or cartilage. For instance, Col1a1 and Col2a1 are responsible for the major extracellular matrix of bone and the cartilaginous template, respectively [27]. Sox9, as a transcription factor, binds to essential sequences in the Col2a1 gene and is essential for chondrocyte differentiation and cartilage formation [36], while Wnt/β-catenin signaling in mesenchymal progenitors favors osteoblast differentiation during vertebrate skeletogenesis and inhibits chondrocyte formation [37]. Therefore, understanding how scaffolds and loaded drugs applied in bone engineering deliver molecular signals of bone formation is crucial.

Ossification patterns also affect angiogenesis, which is vital for providing sufficient nutrition for active cell activities during bone repair or formation. However, mimicking intramembranous ossification may lead to extensive bone matrix on the newly formed bone surface, which hinders the invasion of blood vessels and leads to avascular necrosis and core degradation [38]. This emphasizes the importance of vascularization in maxillofacial bone tissue repair, especially in large bone defects. Studies have shown promising results for promoting angiogenesis in preclinical studies by adding bioactive molecules such as bone morphogenetic protein (BMP)-2 or synthetic ligands to scaffolds. Through enhancing the binding between BMP-2 and BMP-2 type II receptors (BMPR2), S-Gelatin/recombinant human BMP-2 (rhBMP-2) hydrogel could rapidly activate BMPR2 on MSCs to induce differentiation and cytokine secretion to enhance angiogenesis and recapitulate in situ osteogenesis for bone regeneration (Fig. 3) [39,40]. However, we still do not fully understand how embryonic factors affect the final results of maxillofacial bone healing and functions. There have been studies demonstrating the feasibility of endochondral bone formation with MSCs to acquire desirable vascularization, but its application in maxillofacial areas is lacking [41]. Nevertheless, when delivering specific signals for improved osteogenesis and angiogenesis, it is still necessary to consider whether the repair or regeneration of maxillofacial bones should preferentially follow and mimic their native pathway.

2.2.2. Anti-inflammatory and antibacterial property

The anti-inflammatory and antibacterial properties of scaffold biomaterials are critical considerations, given the challenges presented by the bacterial environment of the oral cavity. Macrophages have been identified as playing an active role in bone formation and homeostasis, responding both to biomaterials and to inflammation caused by microbes. However, the neglect of the interaction between materials and immune cells may lead to inconsistencies between in vitro and in vivo evaluations of biomaterials [42,43]. A study evaluating different physicochemical biomaterials for oral and maxillofacial reconstruction found that all the materials tested exhibited similar inflammatory responses and macrophage profiles, indicating a lack of inherent immunomodulation [44]. This underscores the need to consider the immune response when evaluating the osteogenic properties of materials in vitro.

The role of oral microbiomes in bone regeneration is not yet fully understood, but it presents an increased risk of infection at the implantation site. To address this challenge, novel methods are emerging, such as incorporating bioactive elements like antibiotics, antimicrobial peptides, and metal ions into scaffolds to enhance immune response and combat bacterial infection in bone defects [27,45,46]. These approaches offer potential solutions for improving the clinical effectiveness of maxillofacial reconstructive procedures.

2.2.3. Biodegradability

To ensure successful tissue regeneration, it is crucial for the rate of scaffold degradation to match the rate of new tissue formation [47]. The bioabsorption of residual bone engineering materials and volume maintenance of augmented bone are inversely proportional and largely affected by the solubility and acid resistance of the scaffold material [48]. In the maxillofacial region, bone remodeling rates in the maxilla and mandible are 3 and 6 times higher than those in the femur, respectively [23]. Due to the relatively higher bone remodeling properties in the orofacial region, local tissue healing occurs at a relatively faster rate, which may also coincide with the excellent osteogenic ability of orofacial BMSCs. Therefore, it is necessary for the scaffold to degrade at a faster rate that synchronizes with tissue formation. Controlled degradation rates can assist in the spatial and temporal release of drugs and/or biomolecules loaded within the scaffold [7], which should also be coordinated with the stage of tissue formation.

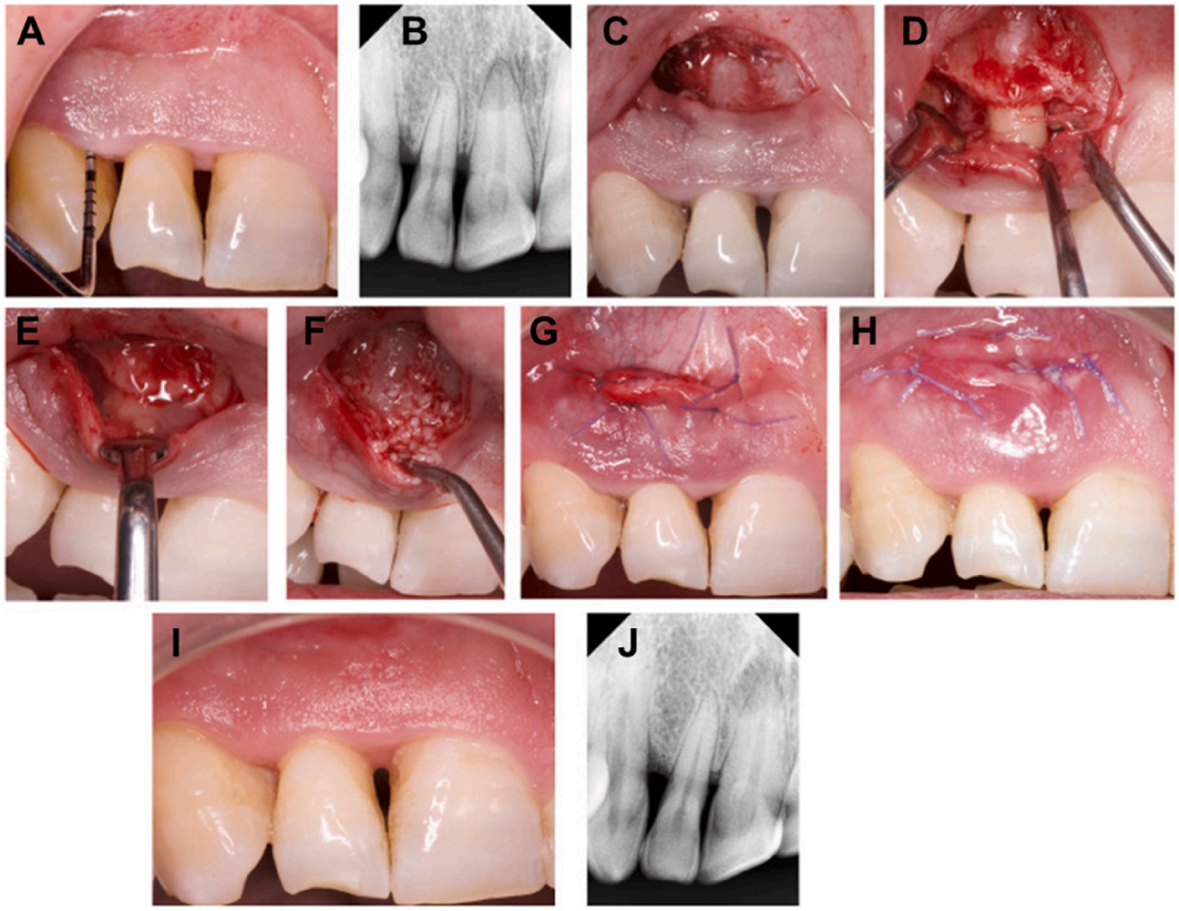

Fig. 8. Application of biomaterial scaffolds in periodontal bone regeneration. (A–B) Pre-operative interproximal probing depth and radiograph. (C–D) Apical incision in the mucosa and elevation of the tissue to expose the bone peaks delimiting the non-contained intrabony defect and coronal traction of the interproximal tissue to expose the supra-alveolar component. (E–F) Application of enamel matrix derivate (EMD) and xenograft bone substitute. (G–H) Suture and wound closure 1 week post-operation. (I–J) One year follow-up. Reprinted with permission from Ref. [87].

3. Advancements in scaffold biomaterials for maxillofacial bone tissue repair

In recent years, many clinical studies have focused on repairing maxillofacial bone defects with various biomaterials, mainly including bone grafts, bone substitutes, bioceramics and APC. There are also biomaterials that only apply to specific conditions, such as autologous teeth in ridge bone preservation and healing after tooth extraction. Most of these materials are safe within the follow-up period, however, study results regarding their efficacy are often contradictory, leaving large room for further exploration. In this part, we summarized recent clinical studies on maxillofacial bone repair with various biomaterials, and pointed out fields that call for further studies to clarify.

3.1. Alveolar bone augmentation

Clinical studies on alveolar bone augmentation have mainly focused on various bone grafts. As summarized in Table 1, most of the trials reported significant augmentation without severe complications, except two studies using an equine xenograft, Bio-Graft® [49,50]. In its early follow-up, soft tissue dehiscence and possible allergy were reported. Although most of the dehiscence cases could be managed, they still predisposed the implant to contamination and subsequent loss [49]. In a longer follow-up period of 28.9 months, graft failure was frequently observed [50]. These problems were not observed with autografts even at a 10-year follow-up, and the dehiscence rate was also lower [49,51]. It might be associated with the low immunocompetence of equine grafts, as indicated by dead cells and significant lymphocyte infiltration 3 months after grafting [50]. Therefore, we believe equine xenografts are not suitable for transplantation in humans.

The harvesting of autologous bone (AB) grafts is associated with extra injury of donor sites (Fig. 4). In order to reduce the need of harvesting AB, Bio-Oss® or cancellous freeze-dried bone allograft (FDBA) are applied with or without AB, and all methods showed good safety and efficacy in alveolar bone augmentation, in so far as a follow-up period up to 3 years [51–56]. But their long-term outcome remains to be further explored.

Notably, although most materials yielded clinically acceptable outcomes, the trials are inconclusive due to limited sample size and follow-up period. Also, many of them are pilot studies with no control groups, so it is hard to compare the efficacy of the subject material to existing treatments.

3.2. Jawbone defect repair

Large cysts and tumors can cause significant jaw defects, which are commonly treated with various bone grafts (Fig. 5, Table 2). The surgical treatment of these large defects is usually quite traumatic, thus complications such as effusion, abscesses and even graft failure might not be attributed to graft materials, but could be caused by patient and surgical factors [59]. Another study applied a 3D-printed PCL/β-TCP implant for complex zygomatico-maxillary defects, and achieved satisfactory early new bone formation rate and implant volume conformity with preoperative design. It proves PCL/β-TCP scaffold is compatible

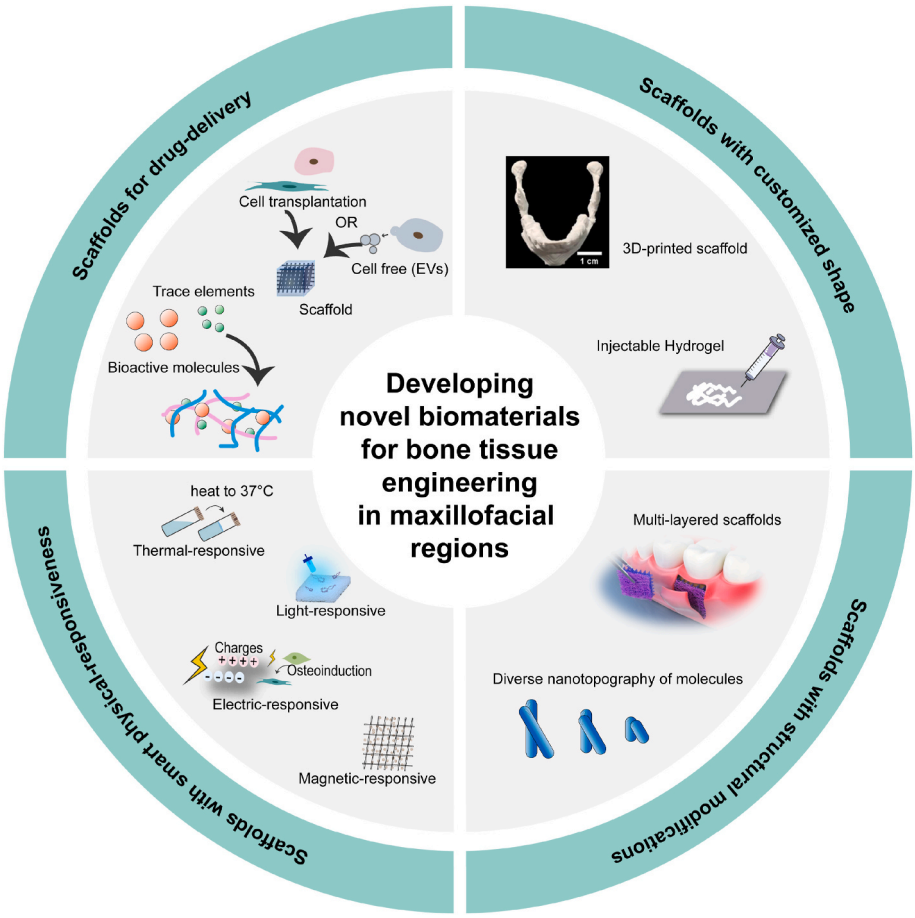

Fig. 9. Developing novel biomaterials for bone tissue engineering in maxillofacial regions.

Table 6
Drugs loaded on scaffolds for maxillofacial bone tissue engineering.

Bioactive molecules	Functions	Examples	Ref.
Growth factors	Promote osteogenesis and angiogenesis	BMPs, vascular endothelial growth factor (VEGF), APCs	[91–98]
Commercially available drugs	Promote osteogenesis, anti-inflammatory and antibiotic effects	Antibiotics, alendronate, aspirin, sildenafil, statins (sitagliptin, atorvastatin, and lovastatin)	[99–104]
Natural herbal extracts	Promote osteogenesis, antibiotic, anti-inflammatory and antioxidative effects	Ginger extracts, garlic extracts, oregano, Croatina grape extracts, hydrocolloid quince seed mucilage	[105–107]
Peptides	Promote osteogenesis and angiogenesis, antibiotic effects	Antimicrobial peptides, osteogenic growth peptides, VEGF-derived peptides	[46,108, 109]
Metal nanoparticles	Antibiotic effects	Silver and copper nanoparticles	[45,110]

with 3D-printing technology while being osteoconductive [60]. It is thus a promising new material for the application in large jaw bone defects.

Overall, clinical studies on biomaterials repairing jawbone defects are scarce, most of them are case reports of low evidence value, and therefore are excluded from this review. We identify an urgent need for more quality clinical studies to elucidate the efficacy of various biomaterials in repairing large jawbone defects.

3.3. Endodontic surgery

Most recent clinical studies on periapical bone defects are focusing on APC (Table 3). The efficacy of APC in promoting periapical bone repair is still questionable. Most studies reported APC addition didn't improve the healing outcome compared with natural healing, or using bioceramics or GBR membrane alone [62–65], except one study on through-and-through apical lesion [66]. However, the use of APC may improve the postoperative quality of life for patients by protecting their speech and sleep function [67]. Therefore, although APC alone may not be a sufficient biomaterial for periapical defect healing, its combined use with bone grafts or bioceramics may be beneficial (Fig. 6).

3.4. Ridge preservation and socket healing

Various biomaterials have been applied to ridge preservation and healing after tooth extraction (Fig. 7, Table 4). Among them, the use of autologous teeth is unique in this condition, because it recycles the extracted teeth as biomaterials. These tooth components have successfully promoted socket healing and ridge preservation. The dentin particles could be absorbed and replaced by bone, and are minimally immunogenic, have good space-making ability, and have a chemical composition similar to autologous bone without causing additional injury to the patient [68]. Therefore, tooth grafts are promising novel biomaterials to be applied in ridge preservation, but currently only few studies are focusing on them. It appears different pre-treating methods of the tooth grafts might have an effect on their performance [69]. But with limited sample size and follow-up period, we cannot draw a

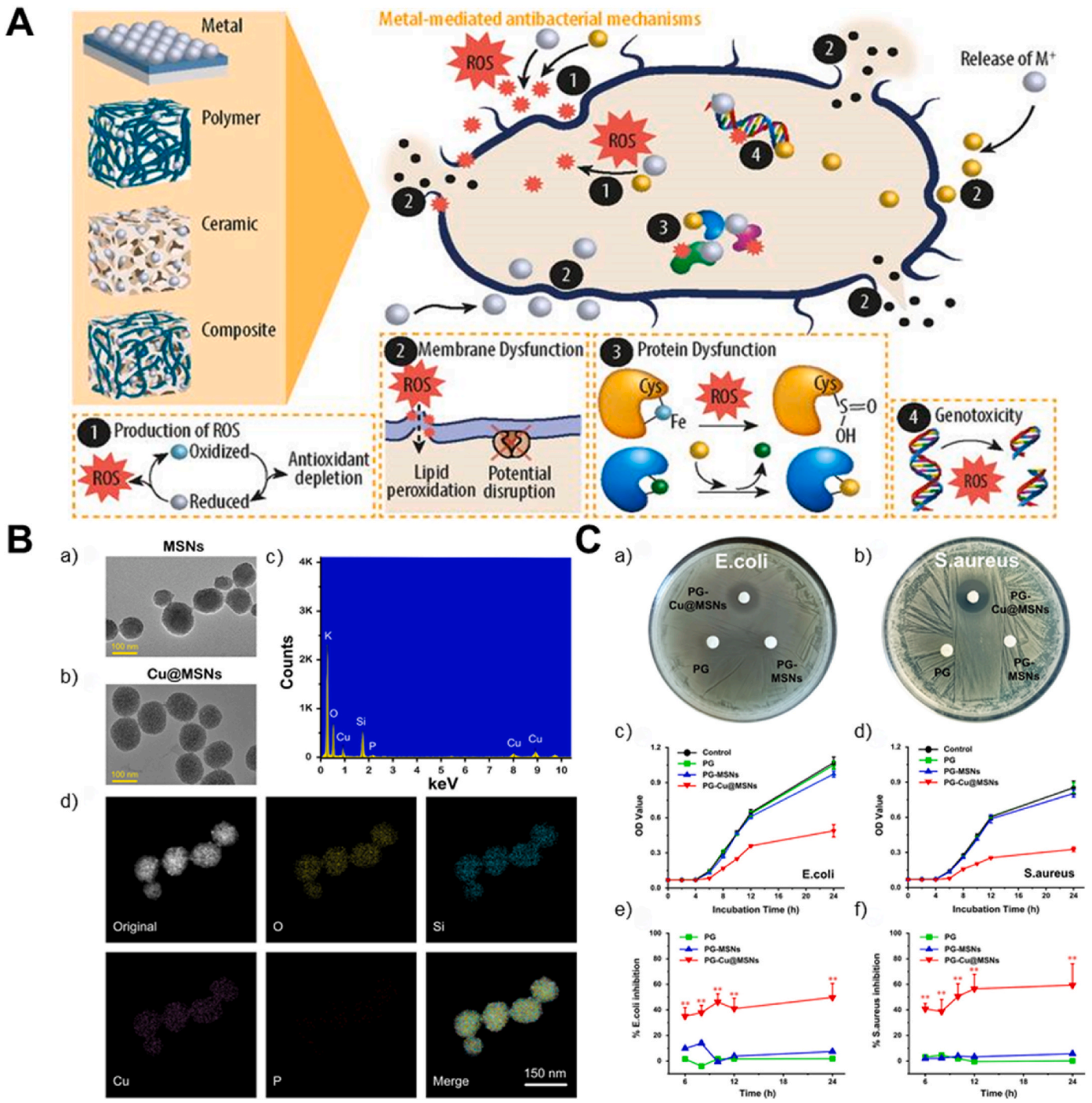

Fig. 10. Anti-bacterial property of metal nanoparticles. (A) Antibacterial mechanisms of metal ions and nanoparticles. Reprinted with permission from Ref. [112]. (B) Transmission electron microscope (TEM) morphologies of mesoporous silica nanoparticles (MSNs) and the prepared copper-loaded MSNs(Cu@MSNs) (a–b), EDS spectrum (d) and mapping images (c) of Cu@MSNs. (C) In vitro antibacterial activity of poly(lactic-co-glycolic acid)/gelatin (PG)-Cu@MSNs scaffolds were shown by inhibition zone (a–b); OD values of bacterial solution (c–d) and bacteria inhibition rates (e–f) of PG, PG-MSNs, and PG-Cu@MSNs scaffolds against E. coli and S. aureus after 24 h of incubation were evaluated. Reprinted with permission from Ref. [110].

definitive conclusion. In total, more quality clinical studies are needed to further evaluate the long-term safety and efficacy and the best pre-treating methods of autologous tooth grafts.

APC's efficacy is debatable. Some studies report APC addition doesn't outperform bone substitute alone or benefit natural healing [70, 71], while others argue it does promote ridge bone preservation or healing [72–74]. Further investigation is needed to clarify the role of APC in ridge bone preservation and healing.

3.5. Periodontal bone regeneration

Differing from the previous conditions, periodontal bone defects caused by periodontitis is characterized by the pervasive inflammation in periodontium.

Most related studies have investigated APC (Table 5). Interestingly, unlike the questionable efficacy shown in periapical lesion and ridge bone preservation and healing, APC demonstrated significant benefits to the regeneration of periodontal tissue [82–85]. We infer this is because

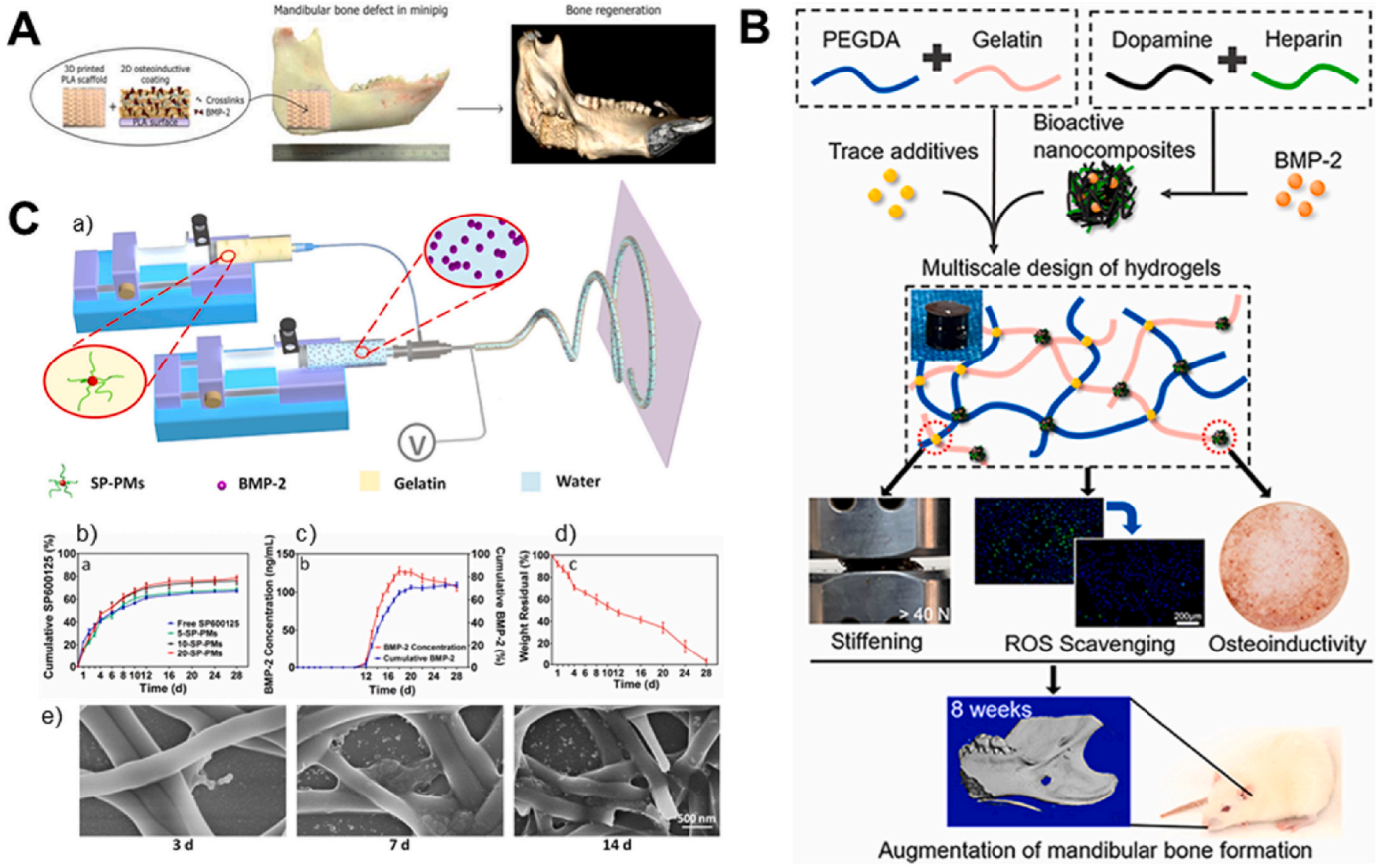

Fig. 11. Methods employed in maxillofacial bone engineering to improve drug delivery ability of solid scaffolds. (A) 3D-printed clinical-grade poly(L-lactide) (PLA) scaffold was coated with polyelectrolyte films to load BMP-2, which promoted bone formation in minipig mandibular defect model. Reprinted with permission from Ref. [93]. (B) Polydopamine-heparin nanoparticles loaded onto a novel hydrogel scaffold achieved sustained release of BMP-2, which scavenges ROS and promotes mandibular bone formation. Reprinted with permission from Ref. [124]. (C) The scaffold was fabricated by coaxial electrospinning (a), and contained polymeric micelles with a c-JNK inhibitor SP600125 (SP-PMs) distributed in the shell to exert an anti-inflammatory effect at the initial stage and BMP-2 incorporated in the core to aid in later osteogenesis, achieving time-programmed and sustained drug release. Release profiles of SP600125 (b) and BMP-2 (c), and in vitro degradation of the nanofiber membrane were shown by weight change (d) and SEM images (e). Reprinted with permission from Ref. [92].

the chronic periodontal inflammation, an important factor driving progressive alveolar bone resorption, can be modulated by the rich growth factors in APC, such as transforming growth factor-β (TGF-β), an immunomodulatory factor. While inflammation in tooth apex is more localized, and usually can be readily removed through endodontic surgery, leaving a comparatively normal environment for healing. Therefore, extra growth factors from APC becomes redundant for an already optimal healing environment free of inflammation, which renders APC ineffective. Same reason applies to the case of ridge bone preservation and socket healing. However, this inference will require more clinical and basic researches to confirm. Clarifying this will also help us better define the best fitted scope of APC application.

Another featured biomaterial in this condition is enamel matrix derivative (EMD). The main components of EMD are enamel matrix proteins secreted by ameloblasts in the Hertwig's epithelial root sheath, which regulate the formation of the periodontal attachment apparatus [86]. Therefore, EMD is particularly suitable for achieving regeneration and reattachment of periodontal tissues, and should be valued as a potential antidote for periodontal damage (Fig. 8). In all studies, significant periodontal regeneration was achieved by using EMD with or without other materials [86,87].

4. Preclinical exploration of novel biomaterials for bone tissue engineering in maxillofacial regions

Although various biomaterials have been applied in clinical practice or clinical trials, there is still a certain distance from the ideal materials. In recent years, studies have tried to develop novel biomaterials dealing with some of the difficulties like bacterial oral environment and irregular bone shape. Enhancement of osteogenesis and angiogenesis is often emphasized as a criterion for evaluating the efficacy of biomaterials in most studies. However, concerns in maxillofacial regions, such as the fast degeneration rate synchronized with tissue formation and long-term performance under mastication, haven't been adequately addressed so far. Here we mainly discuss several frequently used methods in the preclinical exploration of novel biomaterials for maxillofacial bone tissue engineering (Fig. 9).

4.1. Scaffolds for drug-delivery

4.1.1. Bioactive molecules loaded in scaffolds for maxillofacial bone tissue engineering

Various categories of bioactive molecules have been studied for their potential to enhance bone regeneration when loaded onto biomaterials. The following table lists the most frequently loaded molecules in scaffolds for maxillofacial bone tissue engineering in recent years (Table 6).

Given the challenges presented by the bacterial environment of the oral cavity, here we particularly focused on antibacterial drug-loaded scaffolds in maxillofacial regions, which is crucial to fight against infection of implanted scaffolds. Antibiotics, such as metronidazole and ornidazole, are commonly used in periodontal lesions, particularly those caused by anaerobic organisms [99]. A study also demonstrated the

Table 7
Overview of studies using cell therapy for maxillofacial bone tissue regeneration.

Biomaterials	Types of cells loaded	Animal models	Species	Results and critical improvements	Ref.
TCP-PLGA	ADSCs	Mandibular bone defects	Minipig	Improved bone regeneration.	[133]
Gelfoam® based on gelatin	ADSCs	Maxillary bone defects	Rat	Improved bone regeneration.	[130]
Nanostructured fibrin-agarose	ADSCs	Segmental mandibular bone defects	Rat	Improved bone regeneration, poor mechanical properties.	[132]
PCL/TCP	Bone marrow-derived osteoprogenitor cells	Mandibular bone defects	Rabbit	Improved bone regeneration.	[128]
3D-Printed Porous Ti6Al4V Scaffolds + BMSC-containing Matrigels	BMSCs	Mandibular bone defects	Rat	Improved bone regeneration.	[126]
Bioceramics (hydroxypatatite 60 % and β-tricalcium phosphate 40 %)	BMSCs	Mandibular bone defects	Rat	Improved bone regeneration in healthy, diabetic, osteoporotic, or diabetic-osteoporotic rats.	[127]
PCL biomembranes functionalized with BMP-2	BMSCs	Maxillary bone defects	Mouse	Slow release of BMP-2 during bone healing.	[129]
Nanohydroxyapatite/Chitosan/ Gelatin 3D Porous Scaffolds	PDLSCs	Mandibular bone defects	Swine	Improved bone regeneration; structural vascular bone formation.	[143]
Bio-Oss®	GMSCs	Subcutaneous implantation; maxillary bone defects	Mouse; Minipig	Improved bone regeneration.	[144]
3D printed Ti6Al4V scaffolds	retinoic acid induced-iPSCs	Mandibular bone defects	Rat	Improved bone regeneration.	[137]
Tyrosine-derived polycarbonate, E1001(1K)/β-TCP scaffolds	hUVECs + DPSCs	Mandibular bone defects	Rabbit	Improved bone regeneration and angiogenesis.	[131]
Gelatin-conjugated caffeic acid-coated apatite/PLGA scaffold	Trb3-over expressed MSCs	Calvarial bone defects; mandibular bone defects	Mouse; rat	Gene therapy; favor osteoblastogenesis over adipogenesis.	[136]
β-TCP	DMP1 gene-modified BMSCs	Maxillary sinus floor augmentation	Dog	Enhanced mineralization and osseointegration of dental implants; gene therapy.	[135]
Alginate-based hydrogel	GMSC aggregates	Subcutaneous implantation and peri-implantitis model	Mouse; Rat	Photocrosslinking; strong adhesion; enhanced osteogenesis.	[142]
——	3D cell culture with CellSaic	Congenital cleft-jaw model	Rat	DPSCs seemed to be better than BMSCs.	[140]
——	Cell spheroid of BMSCs with osteocytes	Tooth-extraction model	Mouse	Improved bone regeneration.	[141]
——	Hypertrophic cartilage grafts engineered from human fractionated adipose tissue	Mandibular bone defects	Rat	Better than Bio-Oss® DBM granules; simulated endochondral osteogenesis.	[145]

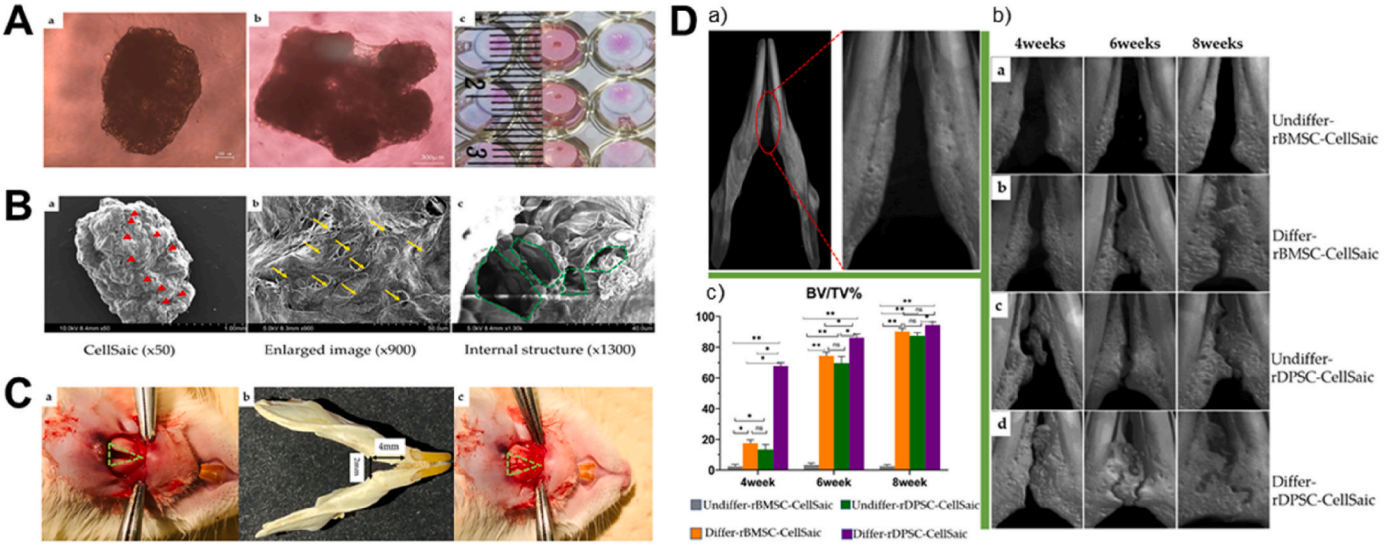

Fig. 12. A novel cell transplantation system CellSaic supports 3D cell culture. (A) Microscopic (a–b) and visual (c) observation of rDPSC-CellSaic. (B) Morphology (a–b) and internal structure (c) of rDPSC-CellSaic shown by SEM. (C) Rat congenital cleft-jaw model: (a) Mandibular defect before surgery; (b) Size of the mandibular defect model (width 2 mm, height 4 mm, depth 1 mm); (c) CellSaics were placed into rat congenital cleft-jaw model. (D) Osteogenesis of the rat congenital cleft-jaw model after 4, 6, and 8 weeks using different CellSaics evaluated by micro-CT (b) and analysis of bone volume/tissue volume (c). The blank control was shown in (a). Reprinted with permission from Ref. [140].

sustained release of metronidazole from a hyaluronic acid sponge loaded with curcumin, a polyphenolic compound, to promote antibacterial, antioxidant, and anti-inflammatory effects for the healing of hard and soft tissues after tooth extraction [111]. Besides, antimicrobial peptides could be easily loaded onto scaffolds through crosslinking [46,108]. They were successfully incorporated into gelatin methacryloyl hydrogels, and provide structural support and exhibit remarkable antimicrobial activity against bacterium involved in peri-implant diseases [108]. Metal nanoparticles, such as silver and copper, have been advocated as a tunable choice to minimize bacterial infection risks. The most probable antibacterial mechanism includes extensive disruption of cellular functions due to damage of cell membrane and the induction of

Table 8
Overview of studies using EVs for maxillofacial bone tissue regeneration.

Biomaterials	Cell sources	Target cells	Animal models	Species	Results and critical improvements	Ref.
collagen membrane	DPSC-EVs	jawbone marrow–derived MSCs	Mandibular bone defects	Rat	a relatively fast wound closure and increased new bone density at the mandible defects.	[149]
PuraMatrix™ hydrogel	DPSC-EVs	ADSCs	Mandibular angle bone defects	Rat	Enhanced bone regeneration.	[155]
Graphene Porous Titanium Alloy Scaffolds	ADSC-EVs	ADSCs	Mandibular bone defects	Rabbit	Enhanced bone regeneration compared with ADSCs alone.	[212]
PEG/DNA hybrid hydrogel	SCAP-EVs	HUVECs and pre-osteoblasts	Mandibular alveolar bone defects	Diabetic rats	Promoting vascularized bone regeneration for diabetic bone defects.	[150]
Collagen hydrogel containing decellularized bone and hydroxyapatite	Osteoblast- EVs	Osteoblasts	Mandibular bone defects	Rabbit	Exerting synergic effects on bone repair with decellularized bone matrix and hydroxyapatite.	[152]
Collagen sponge	DFC-collagenase-released matrix vesicles	DFC	Alveolar bone defects	Rat	Less unhealing areas and more mature bone tissues.	[58]

oxidative stress by metal-mediated reactive oxygen species (ROS) production, culminating in the formation of free radicals and extensive cellular damage of lipids, proteins and DNA by oxidative stress (Fig. 10A) [112]. For example, silver nanoparticles were in situ reduced onto the PLGA/PCL electrospinning scaffold, which led to the reduction of antibiotic load with limited antibiotic resistance and the improvement of bone regeneration in periodontitis mouse model [45]. Another study used copper-loaded mesoporous silica nanoparticles in a PLGA scaffold to enhance antibacterial properties, although only *Escherichia coli* and *Staphylococcus aureus* were selected to test the broad-spectrum antibacterial activity of the scaffold. Further study should pay more attention to evaluate the interactions with oral bacteria (Fig. 10B and C) [110].

4.1.2. Efforts for delivery and sustained release of drugs

The forms of biomaterials have a significant impact on their drug loading and release ability. Collagen and gelatin are among the most used biomaterials clinically as sponge forms, especially in tooth socket. Sponges impregnated with pro-resolving lipid mediator Maresin 1 or growth factor erythropoietin were both shown to promote alveolar ridge regeneration in a rat tooth extraction model, with enhanced osseoinduction and angiogenesis potential [113,114]. Hydrogels like natural polymers are often considered an ideal delivery carrier for controlling the release of loaded drugs to optimize bone engineering efficacy [115,116], whereas solid scaffolds such as synthetic polymers and bioceramics have limited drug delivery convenience. Therefore, some studies developed composite scaffolds combining hydrogels with solid scaffolds like β-TCP or PCL and achieved excellent drug-release performance as well as mechanical strength [117–119]. In the meanwhile, some other methods have been employed in maxillofacial bone engineering to address this challenge as follows.

One such approach is surface coating, which allows for highly homogeneous drug distribution inside all the pores of a solid scaffold. In mandibular defect repair, PLA scaffolds coated with a polyelectrolyte film for BMP-2 delivery achieved a 20- to 75-fold reduction in BMP-2 dosage compared to commercial collagen sponges (Fig. 11A) [93]. However, this method may lead to a burst release at the initial stage, and the homogeneous drug distribution may not address time or spatial-specific drug delivery. Uncontrolled release of growth factors or antibiotics with an initial outburst can lead to unwanted side effects, such as ectopic bone formation, inflammation, and osteolysis [117,120].

Innovative core-shell structure has been proposed as a promising solution [92,121]. Yoon et al. developed a core-shell structured nanofiber scaffold fabricated by coaxial electrospinning for periodontal bone regeneration. The scaffold contained polymeric micelles with a c-JNK inhibitor SP600125 (SP-PMs) distributed in the shell to exert an anti-inflammatory effect at the initial stage and BMP-2 incorporated in the core to aid in later osteogenesis, achieving time-programmed and sustained drug release in a class II furcation model of a dog (Fig. 11C) [92]. Similar core-shell nanofibers were also applied for the sequential and controlled release of tea polyphenols (TP) and AdipoRon (APR) to promote bone regeneration in periodontitis-related alveolar bone defects [121]. It's worth noting that the morphology and diameter of the nanofibers in scaffolds also impacts drug release profile. Nanoparticles enables burst release while sustained release is observed in nanofibers [122,123]. This perspective might be combined in these studies for future improvements.

Microparticles or nanoparticles can also serve as suitable drug carriers [120,124,125]. Polydopamine-heparin nanoparticles loaded onto a novel hydrogel scaffold achieved the sustained release of BMP-2, owing to their affinity with BMP-2 (Fig. 11B) [124].

4.1.3. Delivery of cells and extracellular vehicles (EVs)

Research on MSCs has undergone rapid advancements, driven by their potential in tissue repair. The application of cell therapy for maxillofacial bone regeneration was summarized in Table 7 below. Among different stem cell sources, BMSCs are the most used in maxillofacial bone regeneration. BMSCs loaded on bioceramics or hydrogels have demonstrated superior maxillofacial bone formation in various rat models, including healthy, diabetic, osteoporotic, and diabetic-osteoporotic rats [126–129]. Adipose-derived mesenchymal stem cells (ADSCs) and DPSCs have also garnered attention due to their abundance and ease of collection [130], and demonstrated increased osteogenesis in mandibular bone defects and alveolar bone regeneration [131–133]. Furthermore, preconditioning loaded cells with factors like BMP-2 or gene modification such as sclerostin and DMP-1 have been tried to enhance orofacial bone regeneration [134–138]. However, the utilization of oral BMSCs, which may be the most suitable cell type for maxillofacial bone regeneration, remains relatively uncommon and could be considered in future studies.

Recently, cell aggregates or 3D cell culture techniques have emerged as promising approaches for engineering complex tissues or organs, offering valuable insights for maxillofacial applications [139]. The CellSaic platform, a novel cell transplantation system, supports 3D cell culture and has shown promising bone formation outcome in rat congenital cleft-jaw model, and DPSC-CellSaic seems to be a better source for maxillofacial bone defect repair than BMSC-CellSaic (Fig. 12) [140]. Another study particularly developed ring-shaped bone-like tissue by spheroid co-cultures of BMSCs with osteocytes, which fitted in tooth extraction socket and enhanced alveolar bone regeneration [141]. One significant challenge associated with 3D cell aggregates for maxillofacial bone tissue engineering was the weak adhesion between the hydrogel and the host tissue at the defect site. To address this issue, Hasani-Sadrabadi et al. developed an alginate-based adhesive hydrogel

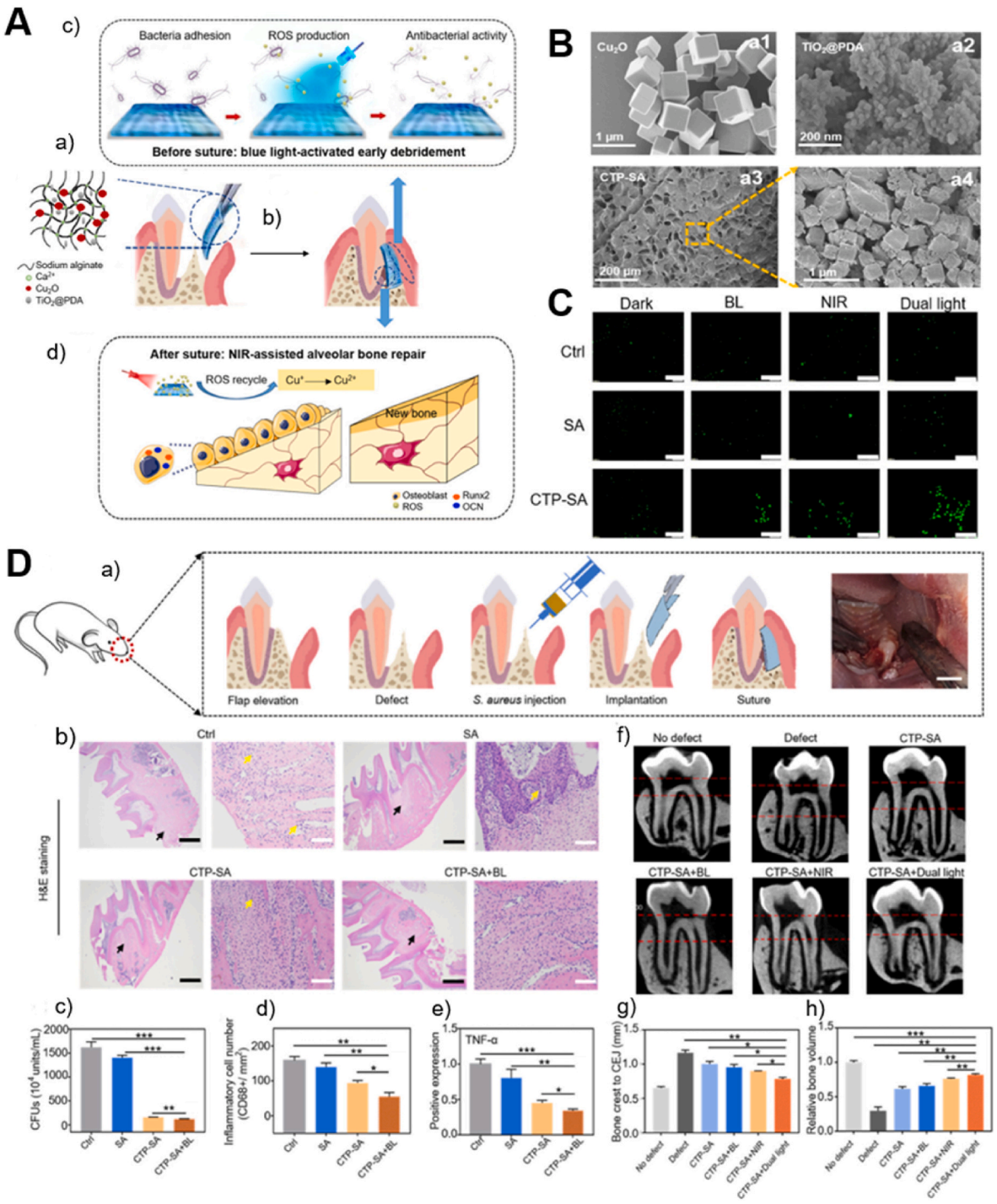

Fig. 13. An injectable sodium alginate hydrogel composite (CTP-SA) doped with cubic cuprous oxide (Cu_2O) and polydopamine-coated titanium dioxide (TiO_2@PDA) nanoparticles. (A) Schematic description of CTP-SA microstructure (a), application procedure (b), broad-spectrum antibacterial capabilities under blue light (BL) irradiation (c), and osteoinduction under near infrared (NIR) irradiation (d). (B) SEM images of the material components. (C) BMSCs produce significantly more ROS on CTP-SA, especially under dual light irradiation. (D) (a) Schematic diagram of in vivo experiment procedure. (b) H&E staining (yellow arrows: inflammatory cells). (c–e) Quantitative statistics of bacteria colonies (c), CD68-positive monocytes (d) and expression of TNF-α gene (e) confirmed the antibacterial property. (f) Micro-CT images of the rats' maxillary first molar. Quantitative statistics of the distance from the bone crest to the CEJ (g) and relative bone volume (h) was used to evaluate the osteogenesis of alveolar bone. Reprinted with permission from Ref. [156].

that could form a dopamine coating, providing an effective delivery vehicle for MSC aggregates and promoting improved adhesion to the host tissue [142]. These advancements in 3D cell culture hold great potential for advancing the field of maxillofacial tissue engineering. However, most of these studies limited in a single cell type, bi-culture and tri-culture of cells might be a promising research direction in the future, enabling the recreation of a more representative in vivo microenvironment.

The paracrine effects of MSCs have garnered significant interest in the field of bone tissue regeneration, with a particular focus on EVs containing proteins and nucleotides [146]. Studies investigating EV-loaded biomaterials for maxillofacial bone regeneration are

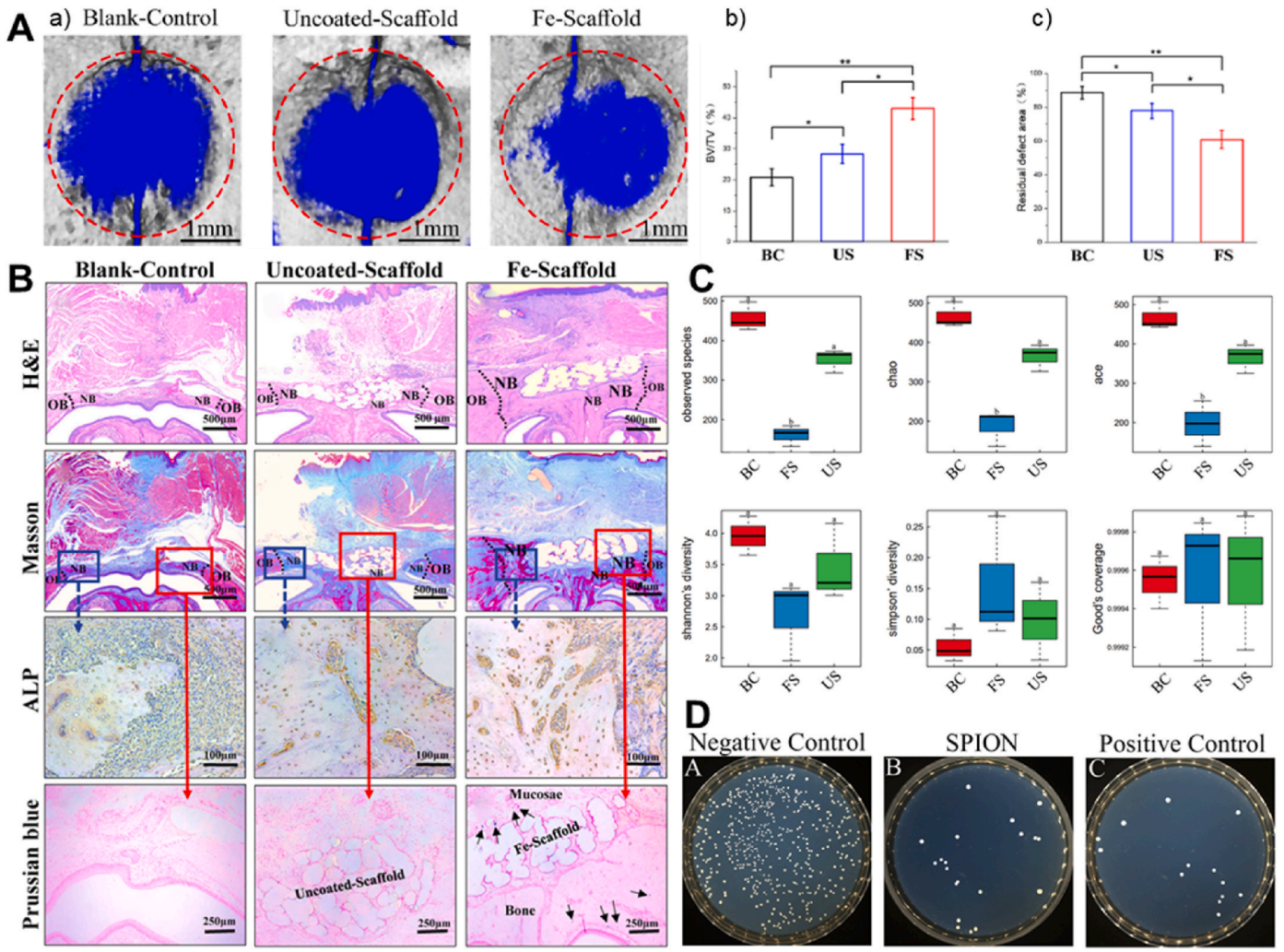

Fig. 14. A 3D-printed PLGA scaffold coated with superparamagnetic iron oxide nanoparticle (SPION) is developed. (A) Micro-CT scans of bone defects (a), relative ratio of bone volume and tissue volume in the defect areas (b), and the residual defect areas (c) were shown. (B) Histological analysis of in vivo bone formation. OB, original bone; NB, new bone. (C) Various analyses showing the scaffold alters the composition of oral microbiota in vivo. BC, blank control; FS, Fe-scaffold; US, uncoated scaffold. (D) In vitro bacteria colony formation test shows the SPION scaffold significantly inhibits the growth of *Clostridium sporogenes*. Reprinted with permission from Ref. [158].

summarized in Table 8. DPSC-derived EVs have been the most used type and could be efficiently uptaken by jawbone marrow-derived MSCs, which have been loaded onto hydrogels, PLLA, or bioceramic, and demonstrated the ability to enhance bone regeneration in all these studies [147–149]. EVs derived from other cell types, such as ADSCs, SCAPs, and osteoblasts, have also shown pro-osteogenic effects in mandibular bone defect models [150–152]. Preconditioning of donor cells could improve the efficacy of EVs. For example, EVs derived from hypoxic BMSCs promoted vascularized bone regeneration more effectively than normoxia BMSC-derived EVs through the miR-210-3p/EFNA3/PI3K pathway [153]. More recently, Yi et al. focused on matrix vesicles (MVs), a subtype of EVs containing mineralization-related biomolecules, and found that MVs obtained from collagenase-digested cell suspensions resulted in the formation of more mature bone tissue when loaded onto a collagen scaffold for optimizing alveolar bone regeneration [154]. In conclusion, as a promising cell-free approach, further investigation is needed to optimize bone regeneration efficacy through cell preconditioning/engineering methods, and deeper thinking is needed to make EVs more suitable for maxillofacial bone regeneration.

4.2. Scaffolds with smart physical-responsiveness

In recent years, there has been an emergence of smart physical-responsive scaffolds, and some studies began to focus on their application in maxillofacial bone engineering. These scaffolds are designed to respond to internal or external stimuli, such as temperature, electricity, and magnetism, thereby enhancing their regenerative efficacy.

4.2.1. Thermal or light-responsive scaffolds

Thermal or light-responsive scaffolds provide a novel approach for shape control and improve biological properties of scaffolds, especially hydrogels. Chitosan hydrogel is a commonly used thermosensitive polymer that undergoes a thermo-irreversible gelation at 37 °C, making it suitable for clinical manipulation. Local injection of chitosan hydrogel in periodontal pockets was found to promote bone formation [101]. In addition, a light-activated gelatin hydrogel was developed by combining biocompatible photoinitiators (triethanolamine/N-vinyl caprolactam/Eosin Y), which could be cured with commercial dental curing systems for easy clinical applications [108]. Recently, light-activated hydrogel with antibacterial functions has also been fabricated for periodontal applications. Xu et al. developed a dual light-sensitive sodium alginate hydrogel composite doped with cubic cuprous oxide (Cu_2O) and

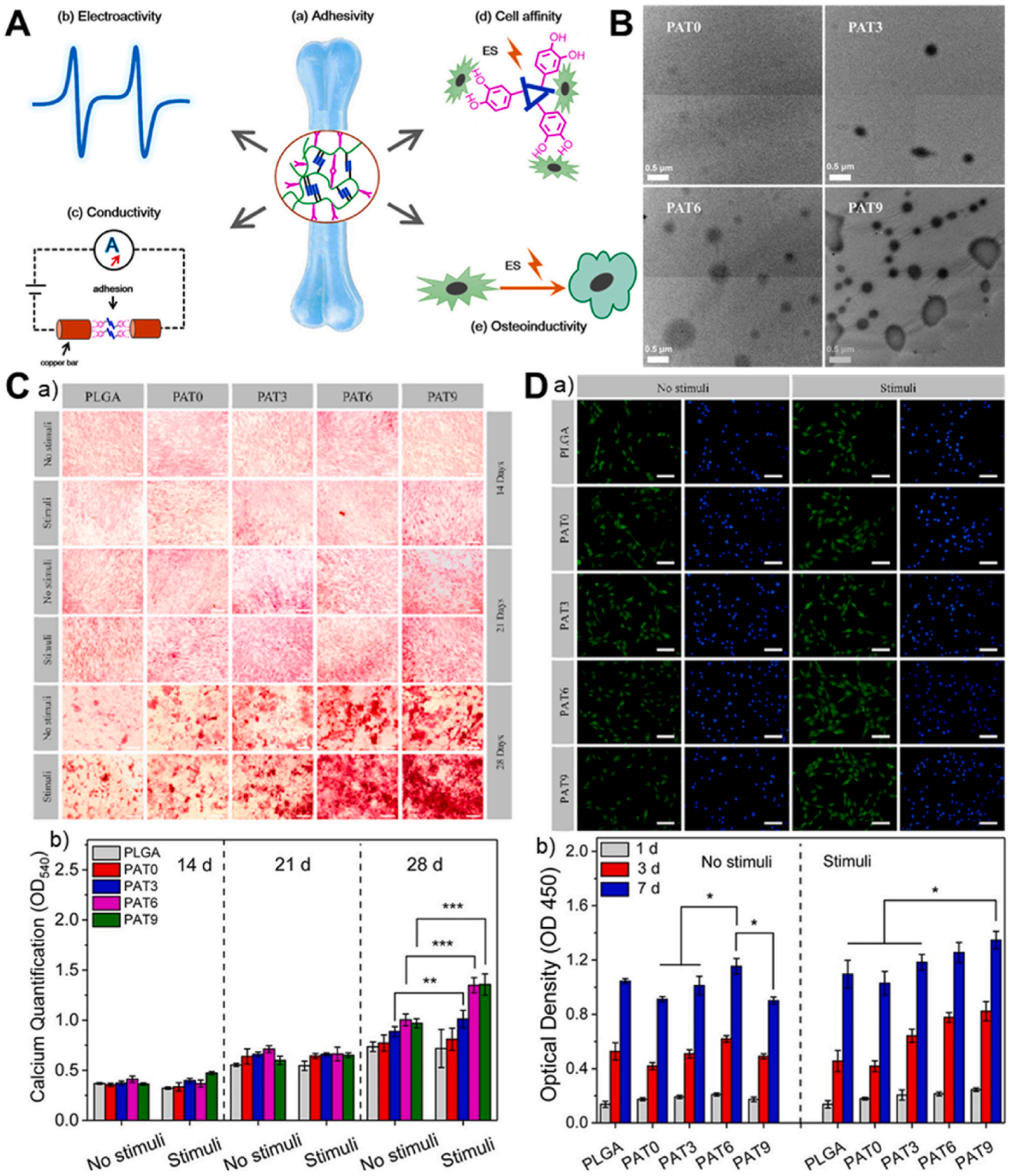

Fig. 15. Inspired by mussel chemistry, a conductive terpolymers poly{[aniline tetramer methacrylamide]-co-[dopamine methacrylamide]-co-[poly(ethylene glycol) methyl ether methacrylate]} [poly(ATMA-co-DOPAMA-co-PEGMA)] is developed, with conductive aniline tetramer (AT) content 3.0, 6.0, and 9.0 mol %, respectively (abbreviated PAT3, 6, 9). (A) Schematic diagram of the functions of the material. (B) TEM for the terpolymer thin films with different AT contents. Dark spots are conductive microregions. (C) Osteoinduction of the scaffolds, with or without electrical stimulation (ES) were shown by Alizarin red staining (a) and relative quantification of calcium nodules (b). (D) Cell adhesion and proliferation rates on the scaffold with or without ES were shown by FITC (green)/DAPI (blue) staining (a) and CCK-8 (b). Reprinted with permission from Ref. [164].

polydopamine-coated titanium dioxide nanoparticles for periodontitis treatments. Excitation with blue light and near-infrared irradiation conferred broad-spectrum antibacterial and osteogenesis capabilities to the biomaterial by accelerating the oxidation of Cu^{+} to Cu^{2+} together with the photothermal effect (Fig. 13) [156]. Another multi-functional and sustained release drug delivery system (MB/BG@LG) was developed by encapsulating methylene blue (MB) and bioactive glass (BG) into the lipid gel (LG) precursor by Macrosol technology, and MB-produced ROS under 660 nm light irradiation can reduce local inflammatory response by inhibiting bacterial growth [157]. These novel methods support minimally invasive surgery by balancing shape control and injectability of hydrogels.

4.2.2. *Magnetic responsive scaffolds*

Magnetic conducting scaffolds commonly employ superparamagnetic iron oxide nanoparticles (SPION) to generate a magnetic field, which can have an impact on oral microbiota. The effects of SPION on microbes can vary depending on factors such as particle size, redox

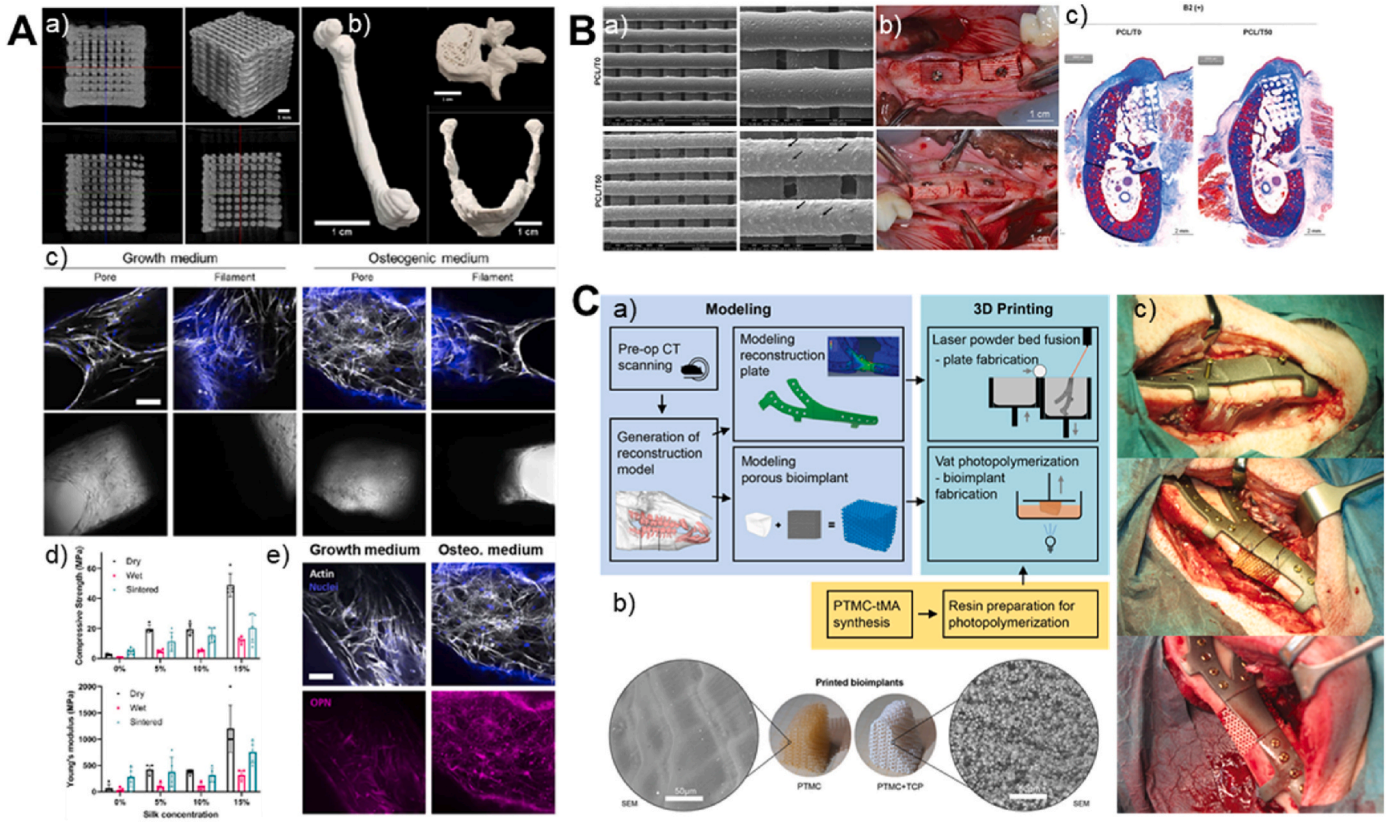

Fig. 16. Examples of 3D-printed scaffolds for bone regeneration. (A) A 3D-printed silk-hydroxyapatite scaffold with controlled macroporosity, regular filament deposition and interconnected pores throughout (a), and can be printed in the shape of various anatomical structures (b). The scaffold supports hMSCs growth (c) and osteogenic differentiation (e). Its mechanical properties are similar to those of trabecular bone (d). Reprinted with permission from Ref. [166]. (B) 3D-printed PCL scaffolds with or without 50 % β-TCP, loaded with rhBMP-2. (a) SEM images showing scaffold microstructure. (b) In vivo implantation of the scaffold in mandibular bone defects. (c) Histological analysis of bone healing. Reprinted with permission from Ref. [165]. (C) The working flow of a patient-specific poly(trimethylene carbonate) (PTMC) and β-TCP bioimplants and reconstruction plates for mandibular defects (a), SEM characterization of the printed bioimplant (b), and the surgical procedure to repair mandibular defects in mini pigs. Reprinted with permission from Ref. [167].

state, and concentration. Additionally, the release of iron ions from SPION contributes to its antibacterial properties by inducing the production of toxic reactive oxygen species [158]. In a study by Jia et al., a 3D-printed PLGA scaffold was coated with SPION using a layer-by-layer assembly technique. The magnetic stimulation resulted in a shift in the composition of oral bacteria, characterized by a decrease in the population of pathogenic bacteria. This shift further facilitated improved bone regeneration in palate bone defects (Fig. 14) [158].

4.2.3. *Electrical responsive scaffolds*

Physiological endogenous electric fields or electrical potential existing within injured tissues play an essential part in bone regeneration [159]. Inspired by this naturally-occurring phenomenon, studies have also demonstrated the positive impact of enhancing the electrical conductivity of materials on maxillofacial bone regeneration, primarily in the context of synthetic scaffolds. Recently, a novel biomimetic ferroelectric BaTiO3/poly(vinylidene fluoridetrifluoroethylene) (BTO/P(VDF-TrFE)) non-resorbable nanocomposite membrane was fabricated to restore the endogeneous electrical microenvironment of alveolar socket, which was implanted with bone grafts and successfully enhanced alveolar ridge regeneration in a mini-pig preclinical model [160]. Graphene and its derivatives have garnered significant attention due to their excellent electrical conductivity, which benefits osteogenic activities and bone formation through two mechanisms: responsiveness to external electrical stimulation and the piezoelectric effect in biomechanical environments [161]. Studies investigated the influence of this pulsed-electromagnetic-field particularly on human alveolar BMSCs and periodontal ligament stem cells (PDLSCs), and found graphene oxide brought positive effects on cell adhesion and osteogenic differentiation [162,163]. These effects may be attributed to enhanced calcium ion efflux, resulting in the upregulation of various signaling pathways, including ERK and Wnt pathways, which are associated with osteogenesis [161]. Furthermore, other conductive polymers, such as terpolymers containing diverse amount of conductive aniline tetramer (AT), have been found to promote adhesion and osteogenic differentiation of preosteoblasts when subjected to electrical stimulation with a square wave (Fig. 15) [164]. Considering that electromagnetic field stimulation has already been commercialized for clinical applications, its potential for future application in maxillofacial bone engineering is promising.

4.3. *Scaffolds with customized shape*

4.3.1. *3D-printed scaffolds*

Achieving tight contact between the graft and recipient site is crucial for improving graft stability and accelerating bone healing by facilitating faster cellular migration [119]. This has led to efforts in developing customized scaffolds to address the irregularities of the maxillofacial region. Various biomaterials have been used for 3D-printed scaffolds, including synthetic polymers, bioceramics, and composite scaffolds (Fig. 16) [106,119,125,165–171]. The design of 3D-printed products relies on computer-operated workflows that ensure specific shapes and accuracy. Bartnikowski et al. introduced a reproducible workflow for 3D-printed PCL scaffolds to regenerate large-sized alveolar bone defects. The dimensional error of these scaffolds was less than 200 μm, making them well-suited for the complex geometry of the

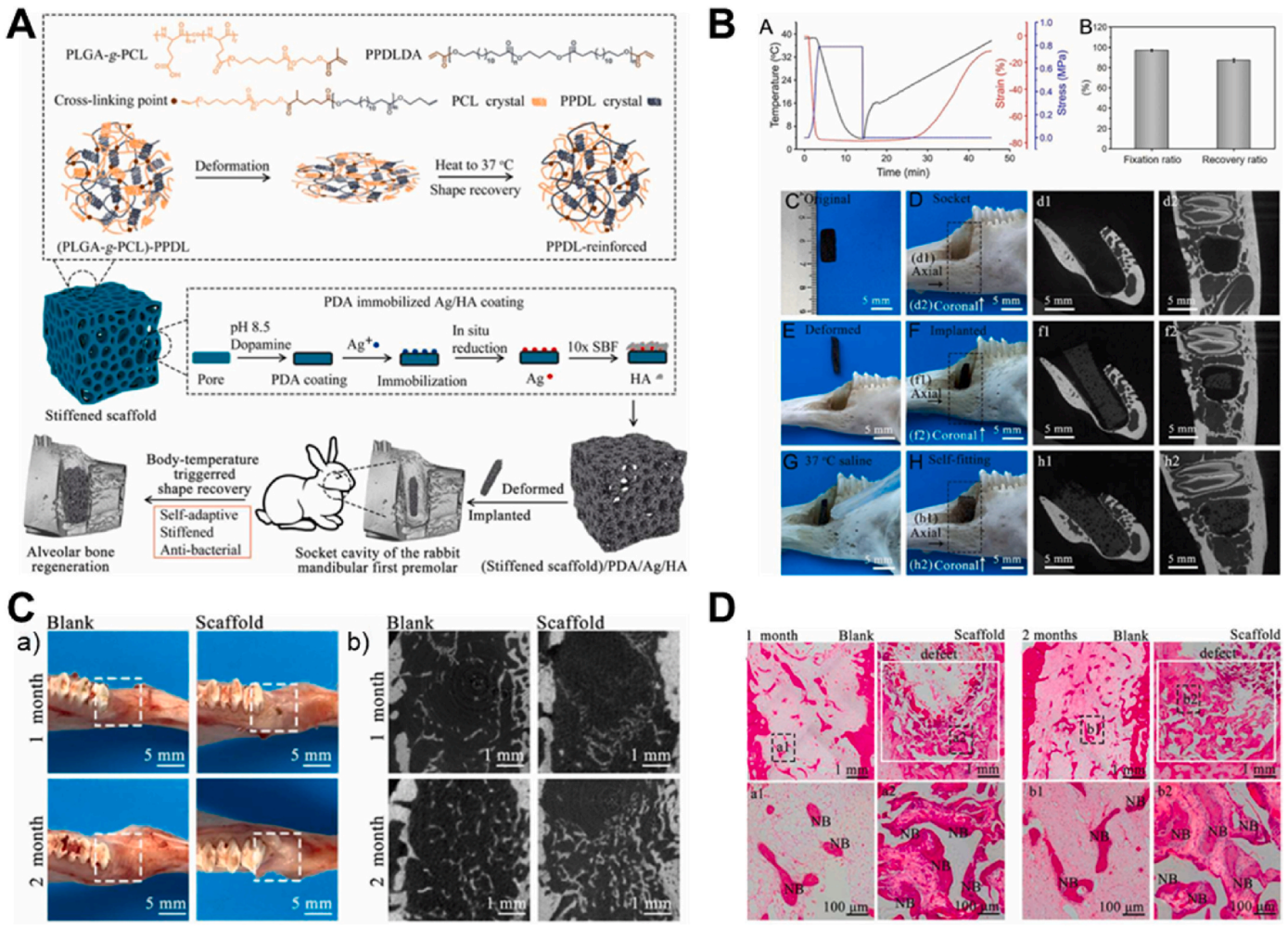

Fig. 17. A porous shape memory self-adaptive stiffened polymer scaffold is fabricated to fit alveolar socket. (A) Illustration of the fabrication and application of the (poly(L-glutamic acid)-g-poly(ε-caprolactone) (PLGA-g-PCL) stiffened scaffold with purposely selected acryloyl chloride-poly(ω-pentadecalactone) (PPDLDA)), showing shape memory and self-adaptive property and anti-bacterial functions for alveolar bone regeneration. (B) Dynamic thermomechanical analyzer curves (A, inset), shape fixation ratio, and recovery ratio (B, inset) of the scaffold were evaluated. In vitro simulation of socket filling was shown (C–H and d1-h1, d2-h2, inset). (C) Rabbits' socket cavity was filled with either scaffold or left unfilled (blank group), and analysis of regenerated alveolar bone was shown in photographs (a) and micro-CT images (b). (D) Histological analysis of regenerated bone in tooth sockets after 1 and 2 months. NB, new bone. Reprinted with permission from Ref. [177].

maxillofacial region [172]. In another study, a layer-by-layer HA-TCP scaffold was fabricated through photocuring a paste material as a bio-ink containing polyfunctional acrylic resins and a photoinitiator. This scaffold exhibited good fit in bone defects in vivo and showed promising outcomes in terms of scaffold osseointegration [169,173]. Besides, given that different parts of the mandible carry different forces, another study designed innovative 3D PCL scaffolds with gradient pore sizes. The upper part of the scaffolds exhibited higher compressive strength while the lower part had lower compressive strength, aligning with the predicted forces on the mandibular symphysis during jaw opening [174], which highlights the unique consideration in maxillofacial bone tissue engineering.

4.3.2. *Injectable hydrogels and scaffolds with plasticity*

When dealing with solid 3D scaffolds, a challenge arises when there are undercuts that hinder insertion. Alternatively, the use of injectable hydrogels and novel bioceramics with plasticity offers a solution to achieve tight contact between the graft and the defect. In a particular study, bioactive glass granules were mixed into CPC paste to create a composite paste that is extrudable and printable, allowing for implants with patient-specific geometries [175]. However, for minimally invasive maxillofacial surgery, it is essential to balance adequate flowability with mechanical strength. To address this, Chiu et al. developed an injectable bone graft material by combining calcium sulfate hemihydrate, TCP, and anhydrous calcium hydrogen phosphate in a suitable ratio. This material exhibits good handling properties, sufficient mechanical strength, and can be squeezed through an 18G needle. However, its biocompatibility and therapeutic effects still require further in vivo exploration [176]. Moreover, Hong et al. introduced a novel injectable CPC scaffold that incorporates ornidazole and PDLSCs. This scaffold exhibits excellent strength, strong antibacterial effects, and osteoinductive ability, demonstrating significant potential for treating bone infections and promoting bone regeneration [99].

However, the same as the majority of commercially available biomaterials for maxillofacial bone regeneration, which are in form of particles, one concern of the injectable biomaterial is the lack in three-dimensional stability. A study tried to handle the challenge by developing porous shape memory self-adaptive stiffened polymer scaffold, which fabricated from copolymerization of biocompatible poly(L-glutamic acid)-g-poly(ε-caprolactone) (PLGA-g-PCL) with purposely selected acryloyl chloride-poly(ω-pentadecalactone) (PPDLDA). The scaffold can be deformed into a compact size, fit well in socket cavity, and recover original shape with a high stiffness in vivo. This is achieved by its higher phase transition temperature than shape recovery

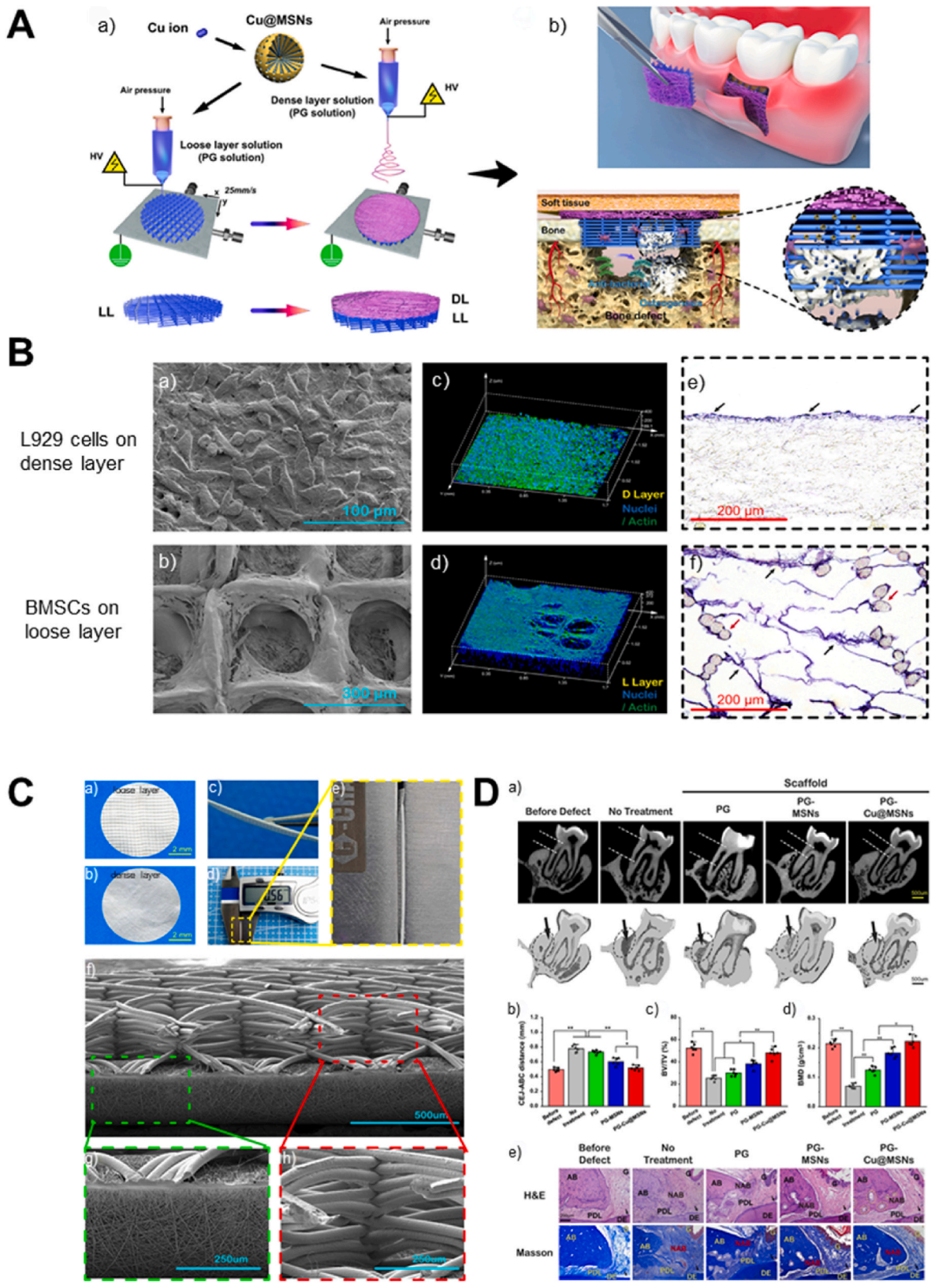

Fig. 18. Multi-layered scaffolds with multiple functions. (A) Preparation process (a) and periodontal application scenario (b) of the bi-layered electrowritten poly (lactic-co-glycolic acid)/gelatin (PG) scaffold loaded with copper-loaded mesoporous silica nanoparticles (Cu@MSNs). DL, dense layer; LL, loose layer. (B) SEM images (a–b), 3D reconstruction of confocal images (c–d), and cross-sectional HE staining (e–f) of L929 cells cultured on the dense layer and BMSCs cultured on the loose layer scaffold. BMSCs could infiltrate into the scaffolds while L929 cells were restricted to the surface of dense layer. (C) Macroscopic appearance (a–c) and thickness measurement (d–e) of the bi-layered scaffold. SEM images (f) with enlarged view showing the cross-sectional appearance of the loose layers (h) and dense layers (g). (D) 2D and 3D micro-CT images showed the superior bone regeneration of PG-Cu@MSNs scaffolds in a rat periodontal defect model (a). Quantitative analysis of micro-CT images (b–d) and histological evaluations (e) of the regenerated bone tissues were shown. Reprinted with permission from Ref. [110].

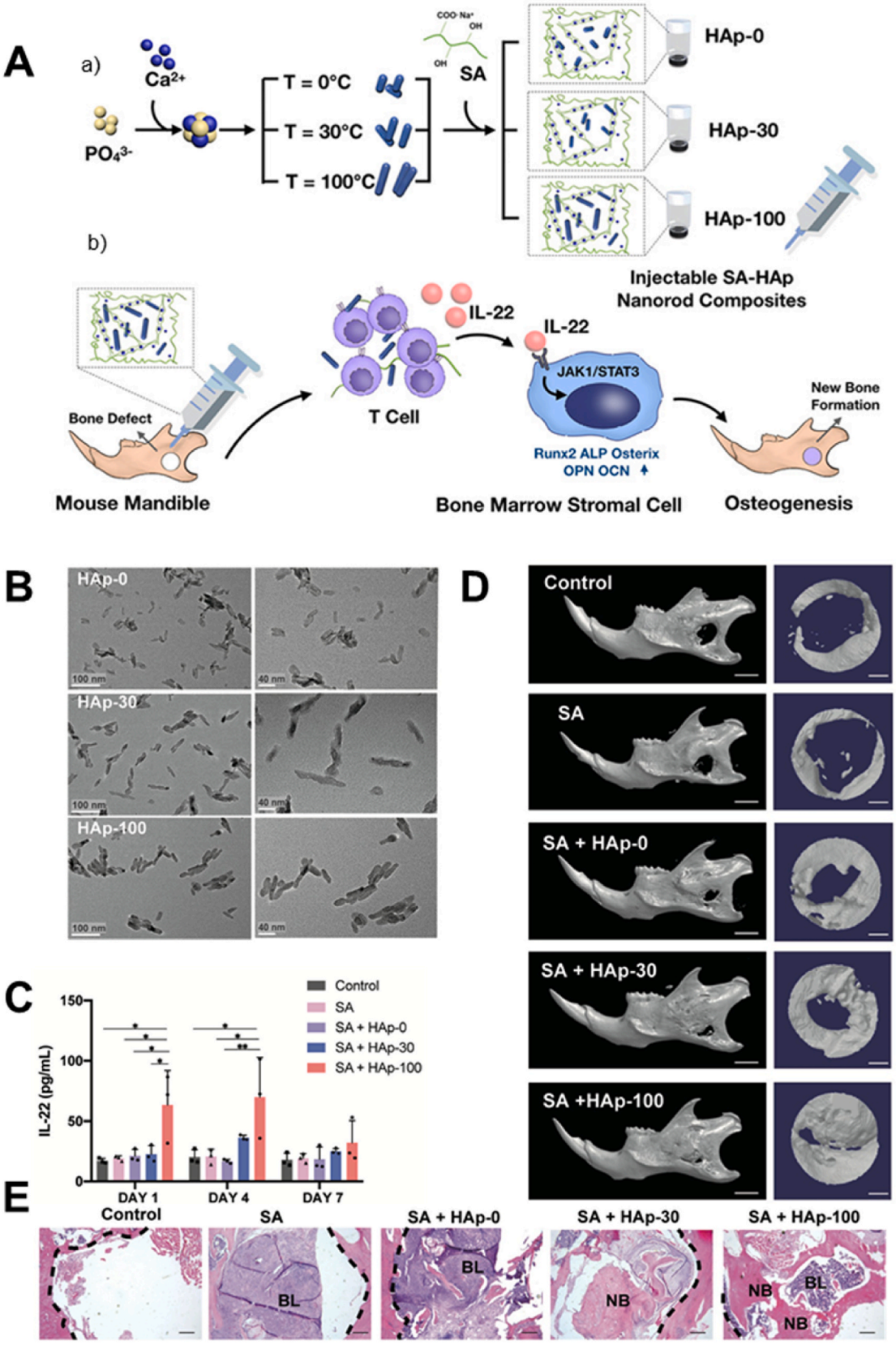

Fig. 19. Biomimetic nanotopography of HA nanorods has a significant impact on their osteogenic and immunomodulation capacities. (A) Schematic illustration of HAp nanorods production by the chemical precipitation approach at different chemical sedimentation temperature (0, 30, and 100 °C, respectively). HAp nanorods dispersed in $CaCl_2$ solution and sodium alginate (SA) solution were mixed at room temperature to obtain a cross-linking hydrogel (a). Injectable SA-Hap nanorods could promote mandibular bone defect repair through T cell-derived IL-22 (b). (B) Representative TEM images of HAp nanorods with different aspect ratios. (C) Concentrations of IL-22 in injured mouse mandibles measured by ELISA on day 1, 4, and 7. (D–E) HE staining and micro-CT showed biomimetic HAp nanorods promote osteogenesis in mouse mandibles with penetrating defects. Reprinted with permission from Ref. [182].

temperature, so as to boosting alveolar bone regeneration (Fig. 17) [177]. Additionally, the combination of hydrogels and solid polymers has also been explored through a printing head deposited methacrylated hyaluronic acid and gelatin-based hydrogels between 3D-printed PCL/TCP frames. Hydrogels facilitated drug loading after photo-crosslinking, while PCL/TCP provided mechanical support [178]. These methods provided promising directions for the development of accurate and controllable customized scaffolds with appropriate strength particularly for maxillofacial regions, further studies are still required to facilitate their clinical translation.

4.4. Scaffolds with structural modifications

Currently, the strategy of structural modification in biomaterials can be applied at multiple scales, including macroscale, microscale, and nanoscale. The improvements at macroscale could be designed according to the diverse needs of different parts, while modifications at micro/nanoscales could control the biological activity of attached cells and biomineralization from a more microscopic perspective. These modifications at different scales could all mimic natural structures, and could be combined and act synergistically in the future, aiming at different needs of maxillofacial scaffolds.

4.4.1. Structural modifications at macroscale

In terms of macrostructure, bi-layered or multi-layered scaffolds were commonly designed following biomimetics so as to fulfill multiple requirements in maxillofacial regions [104]. An example is a PLGA/PCL scaffold composed of three layers: a surface layer containing chlorhexidine, an opposing surface layer containing β-TCP, and a pure PLGA/PCL middle layer. This scaffold integrated the osteoconductive properties of β-TCP and the antibacterial function of chlorhexidine, with the middle layer enhancing its mechanical strength, making it particularly suitable for periodontal regeneration [179]. Similar bi-layered PG-Cu@MSNs scaffolds were also developed with a dense layer designed to resist non-osteoblast (fibroblasts) interference and a loose layer constructed to promote adhesion of BMSCs, facilitate cell-scaffold interaction, and support periodontal bone regeneration (Fig. 18) [110].

Another non-homogeneous structural design is to mimic the natural bone structure. These scaffolds often contain a denser exterior like cortical bone to ensure higher compressive strength and maintain space for bone regeneration, and an interconnected porous center imitating cancellous bone to facilitate cell proliferation, nutrient transport, drug loading and release, and vascularization. Examples as a biphasic PCL scaffold with a core-shell structure and a 3D-printed β-TCP scaffold with bimodal pore geometry were used in maxillofacial regions [106,117]. The excellent mechanical properties of these scaffolds not only facilitated surgical handling but also made it suitable for load-bearing regions such as the mandible.

4.4.2. Structural modifications at microscale

One clinical challenge of mandible reconstruction lies on achieving the complex 3D gridwork formed by the trabeculae, which withstands the forces transmitted during mastication. The spatial microstructure of scaffold influences mechanical properties and material transport properties, which in turn determined local nutrient supply, vascularization, and host-graft interactions [180]. Liu.et al. investigated various arrangements of polymer fibers, revealing the influence of fiber cross angle (FCA) microstructure on the compressive strength and osteogenesis of composite scaffolds, and scaffold with a 90° FCA exhibited the best mechanical performance [180]. The findings provided possibility to design gradient maxillofacial scaffolds by changing the FCAs to adapt different regions without changing the materials to avoid complicated effects.

4.4.3. Structural modifications at nanoscale

Nanotopography has been identified as a contributing factor for the response of immune cells, which becomes critically important under the inflammatory conditions in oral cavity [181]. Therefore, several recent studies focused on nanotopography of biomaterials to enhance their osteoimmunomodulatory properties [182,183]. A hierarchical-structured mineralized scaffold composed of PCL and gelatin nanofibers has been developed, with both anisotropic and isotropic nanofibrous surface topography. The anisotropic regions promoted macrophage M2 polarization by inducing morphological elongation and cytoskeletal changes, while isotropic regions favored osteogenesis, leading to better performance compared with commercial products such as Bio-Oss® and Bio-Guide® in regenerating rat alveolar bone defects [183]. Another study fabricated biomimetic HA structures in scaffolds as nanorods, which closely resemble the nanomorphology of natural HA crystals in bone [109,184]. Among nanorods with diverse aspect ratios, the one crystallized at 100 °C exhibited superior osteogenesis and immunomodulation ability toward IL-22-producing T cells compared to traditional irregular granules, and stimulated repair of injured mandibles (Fig. 19) [182]. These structural modifications at nanoscale could be combined with other improvements when designing scaffolds for maxillofacial bone tissue engineering.

5. Challenges and future prospects

The field of biomaterial sciences and tissue engineering has witnessed remarkable progress, shifting the focus from bone repair to bone regeneration. Numerous studies have explored the use of new biomaterials with enhanced functionality. Maxillofacial bone possesses unique structural, mechanical, and biological properties, and the characteristics of BMSCs also vary depending on the specific location. However, most existing studies investigating novel biomaterials for bone engineering primarily focus on long bones or employ animal models utilizing the cranium, raising a pressing need to summarize existing researches specifically targeting maxillofacial bone defects, and drive more efforts in this field. In this review, we comprehensively examine recent developments in biomaterial scaffolds for maxillofacial bone tissue engineering including both clinical and laboratory studies. By consolidating current knowledge, this review aims to enhance our understanding and stimulate future research in this critical area.

Despite the promising potential of various biomaterials in treating maxillofacial bone defects, current clinical studies face significant limitations that impede progress in assessing the safety and efficacy of these materials. Common limitations include short follow-up periods, small sample sizes, absence of control groups, inconsistent baseline conditions of subjects, and unspecified differences in treatment protocols. Controversies regarding the safety and efficacy of these materials throw challenges in defining their precise indications and contraindications. Consequently, there is a pressing need for high-quality clinical studies to strengthen the evidence base and facilitate more accurate conclusions regarding the use of biomaterials for maxillofacial bone defects.

A wide range of biomaterials for maxillofacial bone tissue engineering are currently being developed with innovative modifications like drug loading, customization, structural modifications, and smart physical responsiveness. Although promising progress has been shown, certain limitations remain to be noted. In terms of study strategies, most experimental studies have primarily focused on evaluating the structure of newly formed bone tissue. However, important questions regarding whether the rate of biomaterial degradation aligns with the rate of tissue regeneration, and whether the newly formed bone can effectively withstand masticatory stress and other physiological conditions, remain unanswered. Additionally, several in vivo studies have utilized extraoral animal models, such as the commonly employed cranial bone defect model. Nevertheless, it is essential to prioritize intraoral models for better assessment of their applications in the maxillofacial region.

Regarding the future development of scaffolds, it is necessary to consider multiple aspects simultaneously during the design process. These aspects include surface topology, load-bearing capacity,

osteogenesis, and other factors that are currently lacking in a significant portion of the existing research. Addressing these aspects will pose challenges for future attempts. Furthermore, tailored biomaterials may be required to fulfill specific functions based on different clinical situations. For example, antibacterial properties may be necessary for periodontal bone regeneration, and diverse load-bearing requirements may exist for different areas within the maxillofacial region. These unique needs in maxillofacial region remain unsolved.

Overall, to translate preclinical studies into clinical applications, practical considerations such as manufacturing, cost, and batch-to-batch consistency of these novel biomaterials must be taken into account. Recently, there have been novel efforts to develop green and environmentally friendly biomaterials by utilizing raw materials such as eggshells, animal waste, agro-waste, plant-derived components, and other natural components [185–188]. These organic wastes are typically low-cost and readily available bioactive materials, and exhibit good in vivo biocompatibility and desirable osteogenic properties, which could be further explored in future studies. With the advancements in fabrication technology and novel modified biomaterials, significant progress in developing biomaterials for maxillofacial bone tissue regeneration is imminent, from the lab bench to chairside practice.

Ethics approval and consent to participate

The manuscript is a review article. The authors declare no experimentation on human or animals were designed.

Declaration of competing interest

The authors declare no conflict of interest.

CRediT authorship contribution statement

Xiangya Huang: Writing – original draft, Writing – review & editing. **Yaxin Lou:** Writing – original draft, Writing – review & editing. **Yihong Duan:** Writing – review & editing. **He Liu:** Writing – review & editing. **Jun Tian:** Writing – review & editing. **Ya Shen:** Supervision, Writing – review & editing. **Xi Wei:** Supervision, Writing – review & editing.

Acknowledgments

This work was supported by National Natural Science Foundation of China (81970974), Guangdong Financial Fund for High-Caliber Hospital Construction (174-2018-XMZC-0001-03-0125/D-04), National Natural Science Foundation of China (82370943), and Key Clinical Technique Program of Guangzhou (2023P-ZD07).

References

[1] A. Vajgel, N. Mardas, B.C. Farias, A. Petrie, R. Cimões, N. Donos, A systematic review on the critical size defect model, Clin. Oral Implants Res. 25 (2014) 879–893, https://doi.org/10.1111/clr.12194.
[2] W. Wang, K.W.K. Yeung, Bone grafts and biomaterials substitutes for bone defect repair: a review, Bioact. Mater. 2 (2017) 224–247, https://doi.org/10.1016/j.bioactmat.2017.05.007.
[3] C.E. Raposo-Amaral, D.F. Bueno, A.B. Almeida, V. Jorgetti, C.C. Costa, C. H. Gouveia, L.C. Vulcano, R.D. Fanganiello, M.R. Passos-Bueno, N. Alonso, Is bone transplantation the gold standard for repair of alveolar bone defects? J. Tissue Eng. 5 (2014), 204173141351935 https://doi.org/10.1177/2041731413519352.
[4] R. Zhao, R. Yang, P.R. Cooper, Z. Khurshid, A. Shavandi, J. Ratnayake, Bone grafts and substitutes in dentistry: a review of current trends and developments, Molecules 26 (2021) 3007, https://doi.org/10.3390/molecules26103007.
[5] D.W. Hutmacher, Scaffolds in tissue engineering bone and cartilage, Biomaterials 21 (2000) 2529–2543, https://doi.org/10.1016/S0142-9612(00)00121-6.
[6] C. Wang, W. Huang, Y. Zhou, L. He, Z. He, Z. Chen, X. He, S. Tian, J. Liao, B. Lu, Y. Wei, M. Wang, 3D printing of bone tissue engineering scaffolds, Bioact. Mater. 5 (2020) 82–91, https://doi.org/10.1016/j.bioactmat.2020.01.004.
[7] H. Zhou, K. Yu, H. Jiang, R. Deng, L. Chu, Y. Cao, Y. Zheng, W. Lu, Z. Deng, B. Liang, A three-in-one strategy: injectable biomimetic porous hydrogels for accelerating bone regeneration via shape-adaptable scaffolds, controllable magnesium ion release, and enhanced osteogenic differentiation, Biomacromolecules 22 (2021) 4552–4568, https://doi.org/10.1021/acs.biomac.1c00842.
[8] X. Chen, B. Tan, Z. Bao, S. Wang, R. Tang, Z. Wang, G. Chen, S. Chen, W.W. Lu, D. Yang, S. Peng, Enhanced bone regeneration via spatiotemporal and controlled delivery of a genetically engineered BMP-2 in a composite hydrogel, Biomaterials 277 (2021), 121117, https://doi.org/10.1016/j.biomaterials.2021.121117.
[9] S. Liu, Y. Wang, B. Ma, J. Shao, H. Liu, S. Ge, Gingipain-responsive thermosensitive hydrogel loaded with SDF-1 facilitates *in situ* periodontal tissue regeneration, ACS Appl. Mater. Interfaces 13 (2021) 36880–36893, https://doi.org/10.1021/acsami.1c08855.
[10] L. Roseti, V. Parisi, M. Petretta, C. Cavallo, G. Desando, I. Bartolotti, B. Grigolo, Scaffolds for bone tissue engineering: state of the art and new perspectives, Mater. Sci. Eng. C. 78 (2017) 1246–1262, https://doi.org/10.1016/j.msec.2017.05.017.
[11] C. Ghayor, F.E. Weber, Osteoconductive microarchitecture of bone substitutes for bone regeneration revisited, Front. Physiol. 9 (2018) 960, https://doi.org/10.3389/fphys.2018.00960.
[12] G. Turco, E. Marsich, F. Bellomo, S. Semeraro, I. Donati, F. Brun, M. Grandolfo, A. Accardo, S. Paoletti, Alginate/hydroxyapatite biocomposite for bone ingrowth: a trabecular structure with high and isotropic connectivity, Biomacromolecules 10 (2009) 1575–1583, https://doi.org/10.1021/bm900154b.
[13] H. Qin, Y. Wei, J. Han, X. Jiang, X. Yang, Y. Wu, Z. Gou, L. Chen, 3D printed bioceramic scaffolds: adjusting pore dimension is beneficial for mandibular bone defects repair, J Tissue Eng Regen Med 16 (2022) 409–421, https://doi.org/10.1002/term.3287.
[14] D. Muallah, P. Sembdner, S. Holtzhausen, H. Meissner, A. Hutsky, D. Ellmann, A. Assmann, M.C. Schulz, G. Lauer, L.M. Kroschwald, Adapting the pore size of individual, 3D-printed CPC scaffolds in maxillofacial surgery, J. Clin. Med. 10 (2021) 2654, https://doi.org/10.3390/jcm10122654.
[15] K. Hayashi, M. Shimabukuro, R. Kishida, A. Tsuchiya, K. Ishikawa, Honeycomb scaffolds capable of achieving barrier membrane-free guided bone regeneration, Mater. Adv. 2 (2021) 7638–7649, https://doi.org/10.1039/d1ma00698c.
[16] Y.S. Zhang, C. Zhu, Y. Xia, Inverse opal scaffolds and their biomedical applications, Adv. Mater. 29 (2017), 1701115, https://doi.org/10.1002/adma.201701115.
[17] L.E. Rustom, T. Boudou, S. Lou, I. Pignot-Paintrand, B.W. Nemke, Y. Lu, M. D. Markel, C. Picart, A.J. Wagoner Johnson, Micropore-induced capillarity enhances bone distribution in vivo in biphasic calcium phosphate scaffolds, Acta Biomater. 44 (2016) 144–154, https://doi.org/10.1016/j.actbio.2016.08.025.
[18] H. Zhang, H. Zhang, Y. Xiong, L. Dong, X. Li, Development of hierarchical porous bioceramic scaffolds with controlled micro/nano surface topography for accelerating bone regeneration, Mater. Sci. Eng. C. 130 (2021), 112437, https://doi.org/10.1016/j.msec.2021.112437.
[19] P. Jiang, Y. Zhang, R. Hu, X. Wang, Y. Lai, G. Rui, C. Lin, Hydroxyapatite-modified micro/nanostructured titania surfaces with different crystalline phases for osteoblast regulation, Bioact. Mater. 6 (2021) 1118–1129, https://doi.org/10.1016/j.bioactmat.2020.10.006.
[20] Q. Liu, W. Wang, L. Zhang, L. Zhao, W. Song, X. Duan, Y. Zhang, Involvement of N-cadherin/β-catenin interaction in the micro/nanotopography induced indirect mechanotransduction, Biomaterials 35 (2014) 6206–6218, https://doi.org/10.1016/j.biomaterials.2014.04.068.
[21] S.J. Hollister, Porous scaffold design for tissue engineering, Nat. Mater. 4 (2005) 518–524, https://doi.org/10.1038/nmat1421.
[22] B. Hesse, M. Langer, P. Varga, A. Pacureanu, P. Dong, S. Schrof, N. Männicke, H. Suhonen, C. Olivier, P. Maurer, G.J. Kazakia, K. Raum, F. Peyrin, Alterations of mass density and 3D osteocyte lacunar properties in bisphosphonate-related osteonecrotic human jaw bone, a synchrotron μCT study, PLoS One 9 (2014), e88481, https://doi.org/10.1371/journal.pone.0088481.
[23] S.S. Huja, F.M. Beck, Bone remodeling in maxilla, mandible, and femur of young dogs, Anat. Rec. 291 (2008) 1–5, https://doi.org/10.1002/ar.20619.
[24] J.D. Currey, Effects of differences in mineralization on the mechanical properties of bone, Phil. Trans. Roy. Soc. Lond. B 304 (1984) 509–518, https://doi.org/10.1098/rstb.1984.0042.
[25] C.E. Misch, Z. Qu, M.W. Bidez, Mechanical properties of trabecular bone in the human mandible: implications for dental implant treatment planning and surgical placement, J. Oral Maxillofac. Surg. 57 (1999) 700–706, https://doi.org/10.1016/s0278-2391(99)90437-8.
[26] V. Wu, M.N. Helder, N. Bravenboer, C.M. ten Bruggenkate, J. Jin, J. Klein Nulend, E.A.J.M. Schulten, Bone tissue regeneration in the oral and maxillofacial region: a review on the application of stem cells and new strategies to improve vascularization, Stem Cell. Int. 2019 (2019) 1–15, https://doi.org/10.1155/2019/6279721.
[27] M. Wang, H. Li, Y. Yang, K. Yuan, F. Zhou, H. Liu, Q. Zhou, S. Yang, T. Tang, A 3D-bioprinted scaffold with doxycycline-controlled BMP2-expressing cells for inducing bone regeneration and inhibiting bacterial infection, Bioact. Mater. 6 (2021) 1318–1329, https://doi.org/10.1016/j.bioactmat.2020.10.022.
[28] P. Leucht, J.B. Kim, R. Amasha, A.W. James, S. Girod, J.A. Helms, Embryonic origin and Hox status determine progenitor cell fate during adult bone regeneration, Development 135 (2008) 2845–2854, https://doi.org/10.1242/dev.023788.
[29] T.L. Aghaloo, T. Chaichanasakul, O. Bezouglaia, B. Kang, R. Franco, S.M. Dry, E. Atti, S. Tetradis, Osteogenic potential of mandibular *vs.* long-bone marrow stromal cells, J. Dent. Res. 89 (2010) 1293–1298, https://doi.org/10.1177/0022034510378427.

[30] S.O. Akintoye, T. Lam, S. Shi, J. Brahim, M.T. Collins, P.G. Robey, Skeletal site-specific characterization of orofacial and iliac crest human bone marrow stromal cells in same individuals, Bone 38 (2006) 758–768, https://doi.org/10.1016/j.bone.2005.10.027.

[31] F. Wang, Y. Zhou, J. Zhou, M. Xu, W. Zheng, W. Huang, W. Zhou, Y. Shen, K. Zhao, Y. Wu, D. Zou, Comparison of intraoral bone regeneration with iliac and alveolar BMSCs, J. Dent. Res. 97 (2018) 1229–1235, https://doi.org/10.1177/0022034518772283.

[32] A.M. Osyczka, M. Damek-Poprawa, A. Wojtowicz, S.O. Akintoye, Age and skeletal sites affect BMP-2 responsiveness of human bone marrow stromal cells, Connect. Tissue Res. 50 (2009) 270–277, https://doi.org/10.1080/03008200902846262.

[33] A. Salhotra, H.N. Shah, B. Levi, M.T. Longaker, Mechanisms of bone development and repair, Nat. Rev. Mol. Cell Biol. 21 (2020) 696–711, https://doi.org/10.1038/s41580-020-00279-w.

[34] A.D. Berendsen, B.R. Olsen, Bone development, Bone. 80 (2015) 14–18, https://doi.org/10.1016/j.bone.2015.04.035.

[35] W.C.W. Chan, Z. Tan, M.K.T. To, D. Chan, Regulation and role of transcription factors in osteogenesis, Int. J. Mol. Sci. 22 (2021) 5445, https://doi.org/10.3390/ijms22115445.

[36] W. Bi, J.M. Deng, Z. Zhang, R.R. Behringer, B. de Crombrugghe, Sox9 is required for cartilage formation, Nat. Genet. 22 (1999) 85–89, https://doi.org/10.1038/8792.

[37] T.F. Day, X. Guo, L. Garrett-Beal, Y. Yang, Wnt/β-catenin signaling in mesenchymal progenitors controls osteoblast and chondrocyte differentiation during vertebrate skeletogenesis, Dev. Cell 8 (2005) 739–750, https://doi.org/10.1016/j.devcel.2005.03.016.

[38] R. Fu, C. Liu, Y. Yan, Q. Li, R.L. Huang, Bone defect reconstruction via endochondral ossification: a developmental engineering strategy, J. Tissue Eng. 12 (2021), 204173142110042, https://doi.org/10.1177/20417314211004211.

[39] Q. Zhang, Y. Liu, J. Li, J. Wang, C. Liu, Recapitulation of growth factor-enriched microenvironment via BMP receptor activating hydrogel, Bioact. Mater. 20 (2023) 638–650, https://doi.org/10.1016/j.bioactmat.2022.06.012.

[40] D. Hao, R. Liu, T.G. Fernandez, C. Pivetti, J.E. Jackson, E.S. Kulubya, H.J. Jiang, H.Y. Ju, W.L. Liu, A. Panitch, K.S. Lam, J.K. Leach, D.L. Farmer, A. Wang, A bioactive material with dual integrin-targeting ligands regulates specific endogenous cell adhesion and promotes vascularized bone regeneration in adult and fetal bone defects, Bioact. Mater. 20 (2023) 179–193, https://doi.org/10.1016/j.bioactmat.2022.05.027.

[41] E.C. Kruijt Spanjer, G.K.P. Bittermann, I.E.M. van Hooijdonk, A.J.W.P. Rosenberg, D. Gawlitta, Taking the endochondral route to craniomaxillofacial bone regeneration: a logical approach? J. Cranio-Maxillo-Fac. Surg. 45 (2017) 1099–1106, https://doi.org/10.1016/j.jcms.2017.03.025.

[42] H. Liu, M. Lin, X. Liu, Y. Zhang, Y. Luo, Y. Pang, H. Chen, D. Zhu, X. Zhong, S. Ma, Y. Zhao, Q. Yang, X. Zhang, Doping bioactive elements into a collagen scaffold based on synchronous self-assembly/mineralization for bone tissue engineering, Bioact. Mater. 5 (2020) 844–858, https://doi.org/10.1016/j.bioactmat.2020.06.005.

[43] S. Franz, S. Rammelt, D. Scharnweber, J.C. Simon, Immune responses to implants – a review of the implications for the design of immunomodulatory biomaterials, Biomaterials 32 (2011) 6692–6709, https://doi.org/10.1016/j.biomaterials.2011.05.078.

[44] M.S. Munerato, C.C. Biguetti, R.B. Parra da Silva, A.C. Rodrigues da Silva, A. C. Zucon Bacelar, J. Lima da Silva, M.C. Rondina Couto, M.A. Húngaro Duarte, J. F. Santiago-Junior, P.S. Bossini, M.A. Matsumoto, Inflammatory response and macrophage polarization using different physicochemical biomaterials for oral and maxillofacial reconstruction, Mater. Sci. Eng. C. 107 (2020), 110229, https://doi.org/10.1016/j.msec.2019.110229.

[45] Y. Qian, X. Zhou, F. Zhang, T.G.H. Diekwisch, X. Luan, J. Yang, Triple PLGA/PCL scaffold modification including silver impregnation, collagen coating, and electrospinning significantly improve biocompatibility, antimicrobial, and osteogenic properties for orofacial tissue regeneration, ACS Appl. Mater. Interfaces 11 (2019) 37381–37396, https://doi.org/10.1021/acsami.9b07053.

[46] M. Li, J. Bai, H. Tao, L. Hao, W. Yin, X. Ren, A. Gao, N. Li, M. Wang, S. Fang, Y. Xu, L. Chen, H. Yang, H. Wang, G. Pan, D. Geng, Rational integration of defense and repair synergy on PEEK osteoimplants via biomimetic peptide clicking strategy, Bioact. Mater. 8 (2022) 309–324, https://doi.org/10.1016/J.BIOACTMAT.2021.07.002.

[47] P.X. Ma, Biomimetic materials for tissue engineering, Adv. Drug Deliv. Rev. 60 (2008) 184–198, https://doi.org/10.1016/j.addr.2007.08.041.

[48] M. Yamada, H. Egusa, Current bone substitutes for implant dentistry, J. Prosthodont. Res. 62 (2018) 152–161, https://doi.org/10.1016/j.jpor.2017.08.010.

[49] A. Ortiz-Vigón, I. Suarez, S. Martínez-Villa, I. Sanz-Martín, J. Bollain, M. Sanz, Safety and performance of a novel collagenated xenogeneic bone block for lateral alveolar crest augmentation for staged implant placement, Clin. Oral Implants Res. 29 (2018) 36–45, https://doi.org/10.1111/clr.13036.

[50] J. Angermair, D.D. Bosshardt, K. Nelson, T.V. Flügge, A. Stricker, T. Fretwurst, Horizontal bone grafting using equine-derived cancellous bone blocks is associated with severe complications: a prospective clinical and histological pilot study, Clin. Oral Implants Res. 31 (2020) 1149–1158, https://doi.org/10.1111/clr.13661.

[51] V. Chappuis, Y. Cavusoglu, D. Buser, T. von Arx, Lateral ridge augmentation using autogenous block grafts and guided bone regeneration: a 10-year prospective case series study, Clin. Implant Dent. Relat. Res. 19 (2017) 85–96, https://doi.org/10.1111/cid.12438.

[52] Y. Ding, L. Wang, K. Su, J. Gao, X. Li, G. Cheng, Horizontal bone augmentation and simultaneous implant placement using xenogeneic bone rings technique: a retrospective clinical study, Sci. Rep. 11 (2021) 4947, https://doi.org/10.1038/s41598-021-84401-8.

[53] G. Işık, M. Özden Yüce, N. Koçak-Topbaş, T. Günbay, Guided bone regeneration simultaneous with implant placement using bovine-derived xenograft with and without liquid platelet-rich fibrin: a randomized controlled clinical trial, Clin. Oral Invest. 25 (2021) 5563–5575, https://doi.org/10.1007/s00784-021-03987-5.

[54] S.M. Meloni, S.A. Jovanovic, I. Urban, E. Baldoni, M. Pisano, M. Tallarico, Horizontal ridge augmentation using GBR with a native collagen membrane and 1:1 ratio of particulate xenograft and autologous bone: a 3-year after final loading prospective clinical study, Clin. Implant Dent. Relat. Res. 21 (2019) 669–677, https://doi.org/10.1111/cid.12808.

[55] F.G.F. Tresguerres, A.R.G. Cortes, G. Hernandez Vallejo, J. Cabrejos-Azama, F. Tamimi, J. Torres, Clinical and radiographic outcomes of allogeneic block grafts for maxillary lateral ridge augmentation: a randomized clinical trial, Clin. Implant Dent. Relat. Res. 21 (2019) 1087–1098, https://doi.org/10.1111/cid.12834.

[56] M. Hashemipoor, N. Asghari, M. Mohammadi, M. Kalantari, M. Arabsolghar, H. Ranjbar, Radiological and histological evaluation of horizontal ridge augmentation using corticocancellous freeze-dried bone allograft with and without autogenous bone: a randomized controlled clinical trial, Clin. Implant Dent. Relat. Res. 22 (2020) 582–592, https://doi.org/10.1111/cid.12935.

[57] R. Vinci, G. Teté, F.R. Lucchetti, P. Capparé, E.F. Gherlone, Implant survival rate in calvarial bone grafts: a retrospective clinical study with 10 year follow-up, Clin. Implant Dent. Relat. Res. 21 (2019) 662–668, https://doi.org/10.1111/cid.12799.

[58] S. Dowlatshahi, C. Chen, H. Zigdon-Giladi, J. Horwitz, C. Ahn, D.M. Kim, E. E. Machtei, Volumetric assessment of changes in the alveolar ridge dimension following guided bone regeneration using a combination freeze-dried bone allograft with collagen membrane or novel resorbable scaffold: a prospective two-center clinical trial, J. Periodontol. 93 (2022) 343–353, https://doi.org/10.1002/jper.21-0006.

[59] Z.H. Ren, T.F. Fan, S. Zhang, H.J. Wu, Nonvascularized iliac bone reconstruction for the mandible without maxillofacial skin scarring, J. Oral Maxillofac. Surg. 78 (2020) 288–294, https://doi.org/10.1016/j.joms.2019.09.012.

[60] W.S. Jeong, Y.C. Kim, J.C. Min, H.J. Park, E.J. Lee, J.H. Shim, J.W. Choi, Clinical application of 3D-printed patient-specific polycaprolactone/beta tricalcium phosphate scaffold for complex zygomatico-maxillary defects, Polymers 14 (2022) 740, https://doi.org/10.3390/polym14040740.

[61] T. Kawai, O. Suzuki, K. Matsui, Y. Tanuma, T. Takahashi, S. Kamakura, Octacalcium phosphate collagen composite facilitates bone regeneration of large mandibular bone defect in humans, J Tissue Eng Regen Med 11 (2017) 1641–1647, https://doi.org/10.1002/term.2110.

[62] N.B. Karan, B. Aricioğlu, Assessment of bone healing after mineral trioxide aggregate and platelet-rich fibrin application in periapical lesions using cone-beam computed tomographic imaging, Clin. Oral Invest. 24 (2020) 1065–1072, https://doi.org/10.1007/s00784-019-03003-x.

[63] N. Meschi, A. Vanhoenacker, O. Strijbos, B. Camargo dos Santos, E. Rubbers, V. Peeters, F. Curvers, M. Van Mierlo, A. Geukens, S. Fieuws, E. Verbeken, P. Lambrechts, Multi-modular bone healing assessment in a randomized controlled clinical trial of root-end surgery with the use of leukocyte- and platelet-rich fibrin and an occlusive membrane, Clin. Oral Invest. 24 (2020) 4439–4453, https://doi.org/10.1007/s00784-020-03309-1.

[64] K.P. Nakkeeran, K. Saravanan, P. Babu, R.R. John, Evaluation of bone regeneration in periapical osseous defects with and without platelet rich plasma, combined calcium sulfate and autologous bone graft – a comparative study, J. Stomatol. Oral. Maxillofac. Surg. 120 (2019) 196–202, https://doi.org/10.1016/j.jormas.2018.11.008.

[65] M. Dhiman, S. Kumar, J. Duhan, P. Sangwan, S. Tewari, Effect of platelet-rich fibrin on healing of apicomarginal defects: a randomized controlled trial, J. Endod. 41 (2015) 985–991, https://doi.org/10.1016/j.joen.2015.04.004.

[66] R. Dhamija, S. Tewari, P. Sangwan, J. Duhan, S. Mittal, Impact of platelet-rich plasma in the healing of through-and-through periapical lesions using 2-dimensional and 3-dimensional evaluation: a randomized controlled trial, J. Endod. 46 (2020) 1167–1184, https://doi.org/10.1016/j.joen.2020.06.004.

[67] D. Soto-Peñaloza, M. Peñarrocha-Diago, J. Cervera-Ballester, M. Peñarrocha-Diago, B. Tarazona-Alvarez, D. Peñarrocha-Oltra, Pain and quality of life after endodontic surgery with or without advanced platelet-rich fibrin membrane application: a randomized clinical trial, Clin. Oral Invest. 24 (2020) 1727–1738, https://doi.org/10.1007/s00784-019-03033-5.

[68] C. Andrade, J. Camino, M. Nally, M. Quirynen, B. Martínez, N. Pinto, Combining autologous particulate dentin, L-PRF, and fibrinogen to create a matrix for predictable ridge preservation: a pilot clinical study, Clin. Oral Invest. 24 (2020) 1151–1160, https://doi.org/10.1007/s00784-019-02922-z.

[69] A. Elfana, S. El-Kholy, H.A. Saleh, K. Fawzy El-Sayed, Alveolar ridge preservation using autogenous whole-tooth versus demineralized dentin grafts: a randomized controlled clinical trial, Clin. Oral Implants Res. 32 (2021) 539–548, https://doi.org/10.1111/clr.13722.

[70] A. Stumbras, P. Galindo-Moreno, G. Januzis, G. Juodzbalys, Three-dimensional analysis of dimensional changes after alveolar ridge preservation with bone substitutes or plasma rich in growth factors: randomized and controlled clinical trial, Clin. Implant Dent. Relat. Res. 23 (2021) 96–106, https://doi.org/10.1111/cid.12950.

[71] X. Wang, M.R. Fok, G. Pelekos, L. Jin, M.S. Tonetti, Increased local concentrations of growth factors from leucocyte- and platelet-rich fibrin do not translate into improved alveolar ridge preservation: an intra-individual mechanistic randomized controlled trial, J. Clin. Periodontol. 49 (2022) 889–898, https://doi.org/10.1111/jcpe.13688.
[72] A.B. Castro, J. Van Dessel, A. Temmerman, R. Jacobs, M. Quirynen, Effect of different platelet-rich fibrin matrices for ridge preservation in multiple tooth extractions: a split-mouth randomized controlled clinical trial, J. Clin. Periodontol. 48 (2021) 984–995, https://doi.org/10.1111/jcpe.13463.
[73] D. Clark, Y. Rajendran, S. Paydar, S. Ho, D. Cox, M. Ryder, J. Dollard, R.T. Kao, Advanced platelet-rich fibrin and freeze-dried bone allograft for ridge preservation: a randomized controlled clinical trial, J. Periodontol. 89 (2018) 379–387, https://doi.org/10.1002/JPER.17-0466.
[74] J.V.D.S. Canellas, R.C. da Costa, R.C. Breves, G.P. de Oliveira, C.M.D. S. Figueredo, R.G. Fischer, A.A. Thole, P.J.D. Medeiros, F.G. Ritto, Tomographic and histomorphometric evaluation of socket healing after tooth extraction using leukocyte- and platelet-rich fibrin: a randomized, single-blind, controlled clinical trial, J. Cranio-Maxillo-Fac. Surg. 48 (2020) 24–32, https://doi.org/10.1016/j.jcms.2019.11.006.
[75] D. Jo, Y. Cho, Y. Seol, Y. Lee, H. Lee, Y. Kim, A randomized controlled clinical trial evaluating efficacy and adverse events of different types of recombinant human bone morphogenetic protein-2 delivery systems for alveolar ridge preservation, Clin. Oral Implants Res. 30 (2019) 396–409, https://doi.org/10.1111/clr.13423.
[76] D. Abellán, L. Barallat, J. Vilarrasa, M. Cabezas, A. Pascual La Rocca, C. Valles, J. Nart, Ridge preservation in molar sites comparing xenograft versus mineralized freeze-dried bone allograft: a randomized clinical trial, Clin. Oral Implants Res. 33 (2022) 511–523, https://doi.org/10.1111/clr.13911.
[77] J. Cha, Y.W. Song, S. Park, R.E. Jung, U. Jung, D.S. Thoma, Alveolar ridge preservation in the posterior maxilla reduces vertical dimensional change: a randomized controlled clinical trial, Clin. Oral Implants Res. 30 (2019) 515–523, https://doi.org/10.1111/clr.13436.
[78] H. Saito, E. Couso-Queiruga, H.J. Shiau, S. Stuhr, H. Prasad, T.V. Allareddy, M. A. Reynolds, G. Avila-Ortiz, Evaluation of poly lactic-co-glycolic acid-coated β-tricalcium phosphate for alveolar ridge preservation: a multicenter randomized controlled trial, J. Periodontol. 92 (2021) 524–535, https://doi.org/10.1002/JPER.20-0360.
[79] M. Debel, S. Toma, B. Vandenberghe, M.C. Brecx, J.F. Lasserre, Alveolar ridge dimensional changes after two socket sealing techniques. a pilot randomized clinical trial, Clin. Oral Invest. 25 (2021) 1235–1243, https://doi.org/10.1007/s00784-020-03428-9.
[80] F. Mercado, C. Vaquette, S. Hamlet, S. Ivanovski, Enamel matrix derivative promotes new bone formation in xenograft assisted maxillary anterior ridge preservation—a randomized controlled clinical trial, Clin. Oral Implants Res. 32 (2021) 732–744, https://doi.org/10.1111/clr.13742.
[81] M.J. Uzeda, R.F. de Brito Resende, S.C. Sartoretto, A.T.N.N. Alves, J.M. Granjeiro, M.D. Calasans-Maia, Randomized clinical trial for the biological evaluation of two nanostructured biphasic calcium phosphate biomaterials as a bone substitute, Clin. Implant Dent. Relat. Res. 19 (2017) 802–811, https://doi.org/10.1111/cid.12516.
[82] A.R. Pradeep, P. Bajaj, N.S. Rao, E. Agarwal, S.B. Naik, Platelet-rich fibrin combined with a porous hydroxyapatite graft for the treatment of 3-wall intrabony defects in chronic periodontitis: a randomized controlled clinical trial, J. Periodontol. 88 (2017) 1288–1296, https://doi.org/10.1902/jop.2012.110722.
[83] P. Bajaj, E. Agarwal, N.S. Rao, S.B. Naik, A.R. Pradeep, N. Kalra, N. Priyanka, M. Kumari, Autologous platelet-rich fibrin in the treatment of 3-wall intrabony defects in aggressive periodontitis: a randomized controlled clinical trial, J. Periodontol. 88 (2017) 1186–1191, https://doi.org/10.1902/jop.2017.120661.
[84] U.P. Nair, R. Shivamurthy, R.R. Nagate, S. Chaturvedi, S.M. Al-Qahtani, M. A. Magbol, S.T. Gokhale, S. Tikare, M. Chaturvedi, Effect of injectable platelet-rich fibrin with a nano-hydroxyapatite bone graft on the treatment of a grade II furcation defect, Bioengineering 9 (2022) 602, https://doi.org/10.3390/bioengineering9110602.
[85] D. Kanoriya, A.R. Pradeep, V. Garg, S. Singhal, Mandibular degree II furcation defects treatment with platelet-rich fibrin and 1% alendronate gel combination: a randomized controlled clinical trial, J. Periodontol. 88 (2017) 250–258, https://doi.org/10.1902/jop.2016.160269.
[86] S. Aslan, N. Buduneli, P. Cortellini, Clinical outcomes of the entire papilla preservation technique with and without biomaterials in the treatment of isolated intrabony defects: a randomized controlled clinical trial, J. Clin. Periodontol. 47 (2020) 470–478, https://doi.org/10.1111/jcpe.13255.
[87] J.A. Moreno Rodríguez, A.J. Ortiz Ruiz, Apical approach in periodontal reconstructive surgery with enamel matrix derivate and enamel matrix derivate plus bone substitutes: a randomized, controlled clinical trial, Clin. Oral Invest. 26 (2022) 2793–2805, https://doi.org/10.1007/s00784-021-04256-1.
[88] J.S. Lee, J.K. Cha, C.S. Kim, Alveolar ridge regeneration of damaged extraction sockets using deproteinized porcine versus bovine bone minerals: a randomized clinical trial, Clin. Implant Dent. Relat. Res. 20 (2018) 729–737, https://doi.org/10.1111/cid.12628.
[89] F. Ferrarotti, F. Romano, M.N. Gamba, A. Quirico, M. Giraudi, M. Audagna, M. Aimetti, Human intrabony defect regeneration with micrografts containing dental pulp stem cells: a randomized controlled clinical trial, J. Clin. Periodontol. 45 (2018) 841–850, https://doi.org/10.1111/jcpe.12931.
[90] M.T. Elbehwashy, M.M. Hosny, A. Elfana, A. Nawar, K. Fawzy El-Sayed, Clinical and radiographic effects of ascorbic acid-augmented platelet-rich fibrin versus platelet-rich fibrin alone in intra-osseous defects of stage-III periodontitis patients: a randomized controlled clinical trial, Clin. Oral Invest. 25 (2021) 6309–6319, https://doi.org/10.1007/s00784-021-03929-1.
[91] C. Vaquette, J. Mitchell, T. Fernandez-Medina, S. Kumar, S. Ivanovski, Resorbable additively manufactured scaffold imparts dimensional stability to extraskeletally regenerated bone, Biomaterials 269 (2021), 120671, https://doi.org/10.1016/j.biomaterials.2021.120671.
[92] X. Liu, W. Zhang, Y. Wang, Y. Chen, J. Xie, J. Su, C. Huang, One-step treatment of periodontitis based on a core-shell micelle-in-nanofiber membrane with time-programmed drug release, J. Contr. Release 320 (2020) 201–213, https://doi.org/10.1016/j.jconrel.2020.01.045.
[93] M. Bouyer, C. Garot, P. Machillot, J. Vollaire, V. Fitzpatrick, S. Morand, J. Boutonnat, V. Josserand, G. Bettega, C. Picart, 3D-printed scaffold combined to 2D osteoinductive coatings to repair a critical-size mandibular bone defect, Mater. Today Bio 11 (2021), 100113, https://doi.org/10.1016/j.mtbio.2021.100113.
[94] S. Cao, S. Li, Y. Geng, K. Kapat, S. Liu, F.H. Perera, Q. Li, H. Terheyden, G. Wu, Y. Che, P. Miranda, M. Zhou, Prefabricated 3D-printed tissue-engineered bone for mandibular reconstruction: a preclinical translational study in primate, ACS Biomater. Sci. Eng. 7 (2021) 5727–5738, https://doi.org/10.1021/acsbiomaterials.1c00509.
[95] S. Nosho, M. Ono, T. Komori, A. Mikai, I. Tosa, K. Ishibashi, Y. Tanaka, A. Kimura-Ono, E.S. Hara, T. Oohashi, T. Kuboki, Preclinical bioequivalence study of E.coli-derived rhBMP-2/β-TCP and autogenous bone in a canine guided-bone regeneration model, J. Prosthodont. Res. 66 (2022) 124–130, https://doi.org/10.2186/jpr.JPR_D_20_00226.
[96] W. Liu, B. Du, S. Tan, Q. Wang, Y. Li, L. Zhou, Vertical guided bone regeneration in the rabbit calvarium using porous nanohydroxyapatite block grafts coated with rhVEGF165 and cortical perforation, Int. J. Nanomed. 15 (2020) 10059–10073, https://doi.org/10.2147/IJN.S268182.
[97] Y. Zhu, N. Cao, Y. Zhang, G. Cao, C. Hao, K. Liu, X. Li, W. Wang, The ability and mechanism of nHAC/CGF in promoting osteogenesis and repairing mandibular defects, Nanomaterials 12 (2022) 212, https://doi.org/10.3390/nano12020212.
[98] Z. Zhao, J. Liu, M.D. Weir, N. Zhang, L. Zhang, X. Xie, C. Zhang, K. Zhang, Y. Bai, H.H.K. Xu, Human periodontal ligament stem cells on calcium phosphate scaffold delivering platelet lysate to enhance bone regeneration, RSC Adv. 9 (2019) 41161–41172, https://doi.org/10.1039/c9ra08336g.
[99] H. Chen, H. Yang, M.D. Weir, A. Schneider, K. Ren, N. Homayounfar, T.W. Oates, K. Zhang, J. Liu, T. Hu, H.H.K. Xu, An antibacterial and injectable calcium phosphate scaffold delivering human periodontal ligament stem cells for bone tissue engineering, RSC Adv. 10 (2020) 40157–40170, https://doi.org/10.1039/d0ra06873j.
[100] G. Xiang, K. Liu, T. Wang, X. Hu, J. Wang, Z. Gao, W. Lei, Y. Feng, T.H. Tao, In situ regulation of macrophage polarization to enhance osseointegration under diabetic conditions using injectable silk/sitagliptin gel scaffolds, Adv. Sci. 8 (2021), 2002328, https://doi.org/10.1002/advs.202002328.
[101] C. Petit, F. Batool, C. Stutz, N. Anton, A. Klymchenko, T. Vandamme, N. Benkirane-Jessel, O. Huck, Development of a thermosensitive statin loaded chitosan-based hydrogel promoting bone healing, Int. J. Pharm. 586 (2020), 119534, https://doi.org/10.1016/j.ijpharm.2020.119534.
[102] S.K. Boda, H. Wang, J.V. John, R.A. Reinhardt, J. Xie, Dual delivery of alendronate and E7-BMP-2 peptide via calcium chelation to mineralized nanofiber fragments for alveolar bone regeneration, ACS Biomater. Sci. Eng. 6 (2020) 2368–2375, https://doi.org/10.1021/acsbiomaterials.0c00145.
[103] L. Lei, Z. Liu, P. Yuan, R. Jin, X. Wang, T. Jiang, X. Chen, Injectable colloidal hydrogel with mesoporous silica nanoparticles for sustained co-release of microRNA-222 and aspirin to achieve innervated bone regeneration in rat mandibular defects, J. Mater. Chem. B 7 (2019) 2722–2735, https://doi.org/10.1039/c9tb00025a.
[104] S. Yahia, I.A. Khalil, I.M. El-Sherbiny, Sandwich-like nanofibrous scaffolds for bone tissue regeneration, ACS Appl. Mater. Interfaces 11 (2019) 28610–28620, https://doi.org/10.1021/acsami.9b06359.
[105] G. Iviglia, E. Torre, C. Cassinelli, M. Morra, Functionalization with a polyphenol-rich pomace extract empowers a ceramic bone filler with in vitro antioxidant, anti-inflammatory, and pro-osteogenic properties, J. Funct. Biomater. 12 (2021) 31, https://doi.org/10.3390/jfb12020031.
[106] S. Bose, D. Banerjee, A.A. Vu, Ginger and garlic extracts enhance osteogenesis in 3D printed calcium phosphate bone scaffolds with bimodal pore distribution, ACS Appl. Mater. Interfaces 14 (2022) 12964–12975, https://doi.org/10.1021/acsami.1c19617.
[107] A.A. Vu, S. Bose, Natural antibiotic oregano in hydroxyapatite-coated titanium reduces osteoclastic bone resorption for orthopedic and dental applications, ACS Appl. Mater. Interfaces 12 (2020) 52383–52392, https://doi.org/10.1021/acsami.0c14993.
[108] E. Shirzaei Sani, R. Portillo Lara, Z. Aldawood, S.H. Bassir, D. Nguyen, A. Kantarci, G. Intini, N. Annabi, An antimicrobial dental light curable bioadhesive hydrogel for treatment of peri-implant diseases, Matter 1 (2019) 926–944, https://doi.org/10.1016/j.matt.2019.07.019.
[109] M. Xiang, M. Zhu, Z. Yang, P. He, J. Wei, X. Gao, J. Song, Dual-functionalized apatite nanocomposites with enhanced cytocompatibility and osteogenesis for periodontal bone regeneration, ACS Biomater. Sci. Eng. 6 (2020) 1704–1714, https://doi.org/10.1021/acsbiomaterials.9b01893.
[110] M. Lian, Y. Han, B. Sun, L. Xu, X. Wang, B. Ni, W. Jiang, Z. Qiao, K. Dai, X. Zhang, A multifunctional electrowritten bi-layered scaffold for guided bone regeneration,

Acta Biomater. 118 (2020) 83–99, https://doi.org/10.1016/j.actbio.2020.08.017.
[111] D. Murgia, G. Angellotti, A. Conigliaro, F. Carfi Pavia, F. D'Agostino, M. Contardi, R. Mauceri, R. Alessandro, G. Campisi, V. De Caro, Development of a multifunctional bioerodible nanocomposite containing metronidazole and curcumin to apply on L-PRF clot to promote tissue regeneration in dentistry, Biomedicines 8 (2020) 425, https://doi.org/10.3390/biomedicines8100425.
[112] M. Godoy-Gallardo, U. Eckhard, L.M. Delgado, Y.J.D. de Roo Puente, M. Hoyos-Nogués, F.J. Gil, R.A. Perez, Antibacterial approaches in tissue engineering using metal ions and nanoparticles: from mechanisms to applications, Bioact. Mater. 6 (2021) 4470–4490, https://doi.org/10.1016/j.bioactmat.2021.04.033.
[113] M. Pandya, M. Saxon, J. Bozanich, C. Tillberg, X. Luan, T.G.H. Diekwisch, The glycoprotein/cytokine erythropoietin promotes rapid alveolar ridge regeneration in vivo by promoting new bone extracellular matrix deposition in conjunction with coupled angiogenesis/osteogenesis, Int. J. Mol. Sci. 22 (2021) 2788, https://doi.org/10.3390/ijms22062788.
[114] C.W. Wang, S.H. Yu, T. Fretwurst, L. Larsson, J.V. Sugai, J. Oh, K. Lehner, Q. Jin, W.V. Giannobile, Maresin 1 promotes wound healing and socket bone regeneration for alveolar ridge preservation, J. Dent. Res. 99 (2020) 930–937, https://doi.org/10.1177/0022034520917903.
[115] B. Divband, M. Aghazadeh, Z.H. Al-qaim, M. Samiei, F.H. Hussein, A. Shaabani, S. Shahi, R. Sedghi, Bioactive chitosan biguanidine-based injectable hydrogels as a novel BMP-2 and VEGF carrier for osteogenesis of dental pulp stem cells, Carbohydr. Polym. 273 (2021), 118589, https://doi.org/10.1016/j.carbpol.2021.118589.
[116] S.W. Jung, J.H. Byun, S.H. Oh, T.H. Kim, J.S. Park, G.J. Rho, J.H. Lee, Multivalent ion-based in situ gelling polysaccharide hydrogel as an injectable bone graft, Carbohydr. Polym. 180 (2018) 216–225, https://doi.org/10.1016/j.carbpol.2017.10.029.
[117] P.T. Sudheesh Kumar, S. Hashimi, S. Saifzadeh, S. Ivanovski, C. Vaquette, Additively manufactured biphasic construct loaded with BMP-2 for vertical bone regeneration: a pilot study in rabbit, Mater. Sci. Eng. C. 92 (2018) 554–564, https://doi.org/10.1016/j.msec.2018.06.071.
[118] H.Z. Lyu, J.H. Lee, The efficacy of rhBMP-2 loaded hydrogel composite on bone formation around dental implants in mandible bone defects of minipigs, Biomater. Res. 24 (2020) 5, https://doi.org/10.1186/s40824-020-0183-9.
[119] J.K. Ku, K.G. Lee, M.S. Ghim, Y.K. Kim, S.H. Park, Y. Park, Y.S. Cho, B.K. Lee, Onlay-graft of 3D printed kagome-structure PCL scaffold incorporated with rhBMP-2 based on hyaluronic acid hydrogel, Biomed. Mater. 16 (2021), 055004, https://doi.org/10.1088/1748-605X/ac0f47.
[120] S. Wu, L. Lei, C. Bao, J. Liu, M.D. Weir, K. Ren, A. Schneider, T.W. Oates, J. Liu, H. H.K. Xu, An injectable and antibacterial calcium phosphate scaffold inhibiting staphylococcus aureus and supporting stem cells for bone regeneration, Mater. Sci. Eng. C. 120 (2021), 111688, https://doi.org/10.1016/j.msec.2020.111688.
[121] Z. He, S. Liu, Z. Li, J. Xu, Y. Liu, E. Luo, Coaxial TP/APR electrospun nanofibers for programmed controlling inflammation and promoting bone regeneration in periodontitis-related alveolar bone defect models, Mater. Today Bio 16 (2022), 100438, https://doi.org/10.1016/j.mtbio.2022.100438.
[122] S.K. Boda, Y. Almoshari, H. Wang, X. Wang, R.A. Reinhardt, B. Duan, D. Wang, J. Xie, Mineralized nanofiber segments coupled with calcium-binding BMP-2 peptides for alveolar bone regeneration, Acta Biomater. 85 (2019) 282–293, https://doi.org/10.1016/j.actbio.2018.12.051.
[123] J. Yoon, H.S. Yang, B.S. Lee, W.R. Yu, Recent progress in coaxial electrospinning: new parameters, various structures, and wide applications, Adv. Mater. 30 (2018), 1704765, https://doi.org/10.1002/adma.201704765.
[124] Y. Wu, X. Li, Y. Sun, X. Tan, C. Wang, Z. Wang, L. Ye, Multiscale design of stiffening and ROS scavenging hydrogels for the augmentation of mandibular bone regeneration, Bioact. Mater. 20 (2023) 111–125, https://doi.org/10.1016/j.bioactmat.2022.05.021.
[125] F. Fahimipour, M. Rasoulianboroujeni, E. Dashtimoghadam, K. Khoshroo, M. Tahriri, F. Bastami, D. Lobner, L. Tayebi, 3D printed TCP-based scaffold incorporating VEGF-loaded PLGA microspheres for craniofacial tissue engineering, Dent. Mater. 33 (2017) 1205–1216, https://doi.org/10.1016/j.dental.2017.06.016.
[126] L. Yu, Y. Wu, J. Liu, B. Li, B. Ma, Y. Li, Z. Huang, Y. He, H. Wang, Z. Wu, G. Qiu, 3D culture of bone marrow-derived mesenchymal stem cells (BMSCs) could improve bone regeneration in 3D-printed porous Ti6Al4V scaffolds, Stem Cell. Int. 2018 (2018) 1–13, https://doi.org/10.1155/2018/2074021.
[127] F. Camacho-Alonso, M. Tudela-Mulero, A. Buendía, J. Navarro, M. Pérez-Sayáns, A. Mercado-Díaz, Bone regeneration in critical-sized mandibular symphysis defects using bioceramics with or without bone marrow mesenchymal stem cells in healthy, diabetic, osteoporotic, and diabetic-osteoporotic rats, Dent. Mater. 38 (2022) 1283–1300, https://doi.org/10.1016/j.dental.2022.06.019.
[128] T. Nuntanaranont, T. Promboot, S. Sutapreyasri, Effect of expanded bone marrow-derived osteoprogenitor cells seeded into polycaprolactone/tricalcium phosphate scaffolds in new bone regeneration of rabbit mandibular defects, J. Mater. Sci. Mater. Med. 29 (2018) 24, https://doi.org/10.1007/s10856-018-6030-z.
[129] C. Stutz, M. Strub, F. Clauss, O. Huck, G. Schulz, H. Gegout, N. Benkirane-Jessel, F. Bornert, S. Kuchler-Bopp, A new polycaprolactone-based biomembrane functionalized with BMP-2 and stem cells improves maxillary bone regeneration, Nanomaterials 10 (2020) 1774, https://doi.org/10.3390/nano10091774.
[130] A. Wofford, A. Bow, S. Newby, S. Brooks, R. Rodriguez, T. Masi, S. Stephenson, J. Gotcher, D.E. Anderson, J. Campbell, M. Dhar, Human fat-derived mesenchymal stem cells xenogenically implanted in a rat model show enhanced new bone formation in maxillary alveolar tooth defects, Stem Cell. Int. 2020 (2020) 1–14, https://doi.org/10.1155/2020/8142938.
[131] W. Zhang, S. Saxena, A. Fakhrzadeh, S. Rudolph, S. Young, J. Kohn, P.C. Yelick, Use of human dental pulp and endothelial cell seeded tyrosine-derived polycarbonate scaffolds for robust in vivo alveolar jaw bone regeneration, Front. Bioeng. Biotechnol. 8 (2020) 796, https://doi.org/10.3389/fbioe.2020.00796.
[132] M.A. Martin-Piedra, B. Gironés-Camarasa, A. España-López, R. Fernández-Valadés Gámez, C. Blanco-Elices, I. Garzón, M. Alaminos, R. Fernández-Valadés, Usefulness of a nanostructured fibrin-agarose bone substitute in a model of severely critical mandible bone defect, Polymers 13 (2021) 3939, https://doi.org/10.3390/polym13223939.
[133] F.A. Probst, R. Fliefel, E. Burian, M. Probst, M. Eddicks, M. Cornelsen, C. Riedl, H. Seitz, A. Aszódi, M. Schieker, S. Otto, Bone regeneration of minipig mandibular defect by adipose derived mesenchymal stem cells seeded tri-calcium phosphate-poly(D,L-lactide-co-glycolide) scaffolds, Sci. Rep. 10 (2020) 2062, https://doi.org/10.1038/s41598-020-59038-8.
[134] S. Maillard, L. Sicard, C. Andrique, C. Torrens, J. Lesieur, B. Baroukh, T. Coradin, A. Poliard, L. Slimani, C. Chaussain, Combining sclerostin neutralization with tissue engineering: an improved strategy for craniofacial bone repair, Acta Biomater. 140 (2022) 178–189, https://doi.org/10.1016/j.actbio.2021.11.046.
[135] D. Ma, Y. Wang, Y. Chen, G. Yang, X. Liu, Promoting osseointegration of dental implants in dog maxillary sinus floor augmentation using dentin matrix protein 1-transduced bone marrow stem cells, Tissue Eng Regen Med 17 (2020) 705–715, https://doi.org/10.1007/s13770-020-00277-1.
[136] J. Fan, C.S. Lee, S. Kim, X. Zhang, J. Pi-Anfruns, M. Guo, C. Chen, M. Rahnama, J. Li, B.M. Wu, T.L. Aghaloo, M. Lee, Trb3 controls mesenchymal stem cell lineage fate and enhances bone regeneration by scaffold-mediated local gene delivery, Biomaterials 264 (2021), 120445, https://doi.org/10.1016/j.biomaterials.2020.120445.
[137] L. Yu, Y. Yang, B. Zhang, X. Bai, Q. Fei, L. Zhang, Rapid human-derived iPSC osteogenesis combined with three-dimensionally printed Ti6Al4V scaffolds for the repair of bone defects, J. Cell. Physiol. 235 (2020) 9763–9772, https://doi.org/10.1002/jcp.29788.
[138] A. Bakopoulou, A. Georgopoulou, I. Grivas, C. Bekiari, O. Prymak, K. Loza, M. Epple, G.C. Papadopoulos, P. Koidis, M. Chatzinikolaidou, Dental pulp stem cells in chitosan/gelatin scaffolds for enhanced orofacial bone regeneration, Dent. Mater. 35 (2019) 310–327, https://doi.org/10.1016/j.dental.2018.11.025.
[139] J. Hoarau-Véchot, A. Rafii, C. Touboul, J. Pasquier, Halfway between 2D and animal models: are 3D cultures the ideal tool to study cancer-microenvironment interactions? Int. J. Mol. Sci. 19 (2018) 181, https://doi.org/10.3390/ijms19010181.
[140] J. Lyu, Y. Hashimoto, Y. Honda, N. Matsumoto, Comparison of osteogenic potentials of dental pulp and bone marrow mesenchymal stem cells using the new cell transplantation platform, CellSaic, in a rat congenital cleft-jaw model, Int. J. Mol. Sci. 22 (2021) 9478, https://doi.org/10.3390/ijms22179478.
[141] Y.H. Zhou, Y. Guo, J.Y. Zhu, C.Y. Tang, Y.Q. Zhao, H.D. Zhou, Spheroid co-culture of BMSCs with osteocytes yields ring-shaped bone-like tissue that enhances alveolar bone regeneration, Sci. Rep. 12 (2022), 14636, https://doi.org/10.1038/s41598-022-18675-x.
[142] M.M. Hasani-Sadrabadi, P. Sarrion, S. Pouraghaei, Y. Chau, S. Ansari, S. Li, T. Aghaloo, A. Moshaverinia, An engineered cell-laden adhesive hydrogel promotes craniofacial bone tissue regeneration in rats, Sci. Transl. Med. 12 (2020), eaay6853, https://doi.org/10.1126/scitranslmed.aay6853.
[143] Q. Zhao, G. Li, T. Wang, Y. Jin, W. Lu, J. Ji, Human periodontal ligament stem cells transplanted with nanohydroxyapatite/chitosan/gelatin 3D porous scaffolds promote jaw bone regeneration in swine, Stem Cell. Dev. 30 (2021) 548–559, https://doi.org/10.1089/scd.2020.0204.
[144] A. Shi, A. Heinayati, D. Bao, H. Liu, X. Ding, X. Tong, L. Wang, B. Wang, H. Qin, Small molecule inhibitor of TGF-β signaling enables robust osteogenesis of autologous GMSCs to successfully repair minipig severe maxillofacial bone defects, Stem Cell Res. Ther. 10 (2019) 172, https://doi.org/10.1186/s13287-019-1281-2.
[145] C. Cheng, M. Chaaban, G. Born, I. Martin, Q. Li, D.J. Schaefer, C. Jaquiery, A. Scherberich, Repair of a rat mandibular bone defect by hypertrophic cartilage grafts engineered from human fractionated adipose tissue, Front. Bioeng. Biotechnol. 10 (2022), 841690, https://doi.org/10.3389/fbioe.2022.841690.
[146] S.H.S. Tan, J.R.Y. Wong, S.J.Y. Sim, C.K.E. Tjio, K.L. Wong, J.R.J. Chew, J.H. P. Hui, W.S. Toh, Mesenchymal stem cell exosomes in bone regenerative strategies—a systematic review of preclinical studies, Mater. Today Bio 7 (2020), 100067, https://doi.org/10.1016/j.mtbio.2020.100067.
[147] Y. Imanishi, M. Hata, R. Matsukawa, A. Aoyagi, M. Omi, M. Mizutani, K. Naruse, S. Ozawa, M. Honda, T. Matsubara, J. Takebe, Efficacy of extracellular vesicles from dental pulp stem cells for bone regeneration in rat calvarial bone defects, Inflamm. Regen. 41 (2021) 12, https://doi.org/10.1186/s41232-021-00163-w.
[148] W.B. Swanson, Z. Zhang, K. Xiu, T. Gong, M. Eberle, Z. Wang, P.X. Ma, Scaffolds with controlled release of pro-mineralization exosomes to promote craniofacial bone healing without cell transplantation, Acta Biomater. 118 (2020) 215–232, https://doi.org/10.1016/j.actbio.2020.09.052.
[149] A.E. Lee, J.G. Choi, S.H. Shi, P. He, Q.Z. Zhang, A.D. Le, DPSC-derived extracellular vesicles promote rat jawbone regeneration, J. Dent. Res. 102 (2023) 313–321, https://doi.org/10.1177/00220345221133716.
[150] X. Jing, S. Wang, H. Tang, D. Li, F. Zhou, L. Xin, Q. He, S. Hu, T. Zhang, T. Chen, J. Song, Dynamically bioresponsive DNA hydrogel incorporated with dual-functional stem cells from apical papilla-derived exosomes promotes diabetic bone regeneration, ACS Appl. Mater. Interfaces 14 (2022) 16082–16099, https://doi.org/10.1021/acsami.2c02278.
[151] X. Sun, S. Yang, S. Tong, S. Guo, Study on exosomes promoting the osteogenic differentiation of ADSCs in graphene porous titanium alloy scaffolds, Front.

Bioeng. Biotechnol. 10 (2022), 905511, https://doi.org/10.3389/fbioe.2022.905511.
[152] A. Emami, T. Talaei-Khozani, S. Tavanafar, N. Zareifard, N. Azarpira, Z. Vojdani, Synergic effects of decellularized bone matrix, hydroxyapatite, and extracellular vesicles on repairing of the rabbit mandibular bone defect model, J. Transl. Med. 18 (2020) 361, https://doi.org/10.1186/s12967-020-02525-3.
[153] Y. Zhuang, M. Cheng, M. Li, J. Cui, J. Huang, C. Zhang, J. Si, K. Lin, H. Yu, Small extracellular vesicles derived from hypoxic mesenchymal stem cells promote vascularized bone regeneration through the miR-210-3p/EFNA3/PI3K pathway, Acta Biomater. 150 (2022) 413–426, https://doi.org/10.1016/j.actbio.2022.07.015.
[154] G. Yi, S. Zhang, Y. Ma, X. Yang, F. Huo, Y. Chen, B. Yang, W. Tian, Matrix vesicles from dental follicle cells improve alveolar bone regeneration via activation of the PLC/PKC/MAPK pathway, Stem Cell Res. Ther. 13 (2022) 41, https://doi.org/10.1186/s13287-022-02721-6.
[155] Q. Jin, P. Li, K. Yuan, F. Zhao, X. Zhu, P. Zhang, Z. Huang, Extracellular vesicles derived from human dental pulp stem cells promote osteogenesis of adipose-derived stem cells via the MAPK pathway, J. Tissue Eng. 11 (2020), 204173142097556, https://doi.org/10.1177/2041731420975569.
[156] Y. Xu, S. Zhao, Z. Weng, W. Zhang, X. Wan, T. Cui, J. Ye, L. Liao, X. Wang, Jelly-inspired injectable guided tissue regeneration strategy with shape auto-matched and dual-light-defined antibacterial/osteogenic pattern switch properties, ACS Appl. Mater. Interfaces 12 (2020) 54497–54506, https://doi.org/10.1021/acsami.0c18070.
[157] Y. Chen, F. Dai, T. Deng, L. Wang, Y. Yang, C. He, Q. Liu, J. Wu, F. Ai, L. Song, An injectable MB/BG@LG sustained release lipid gel with antibacterial and osteogenic properties for efficient treatment of chronic periodontitis in rats, Mater. Today Bio 21 (2023), 100699, https://doi.org/10.1016/j.mtbio.2023.100699.
[158] L. Jia, Z. Yang, L. Sun, Q. Zhang, Y. Guo, Y. Chen, Y. Dai, Y. Xia, A three-dimensional-printed SPION/PLGA scaffold for enhanced palate-bone regeneration and concurrent alteration of the oral microbiota in rats, Mater. Sci. Eng. C. 126 (2021), 112173, https://doi.org/10.1016/j.msec.2021.112173.
[159] Y. Li, Y. Meng, Y. Bai, Y. Wang, J. Wang, B. Heng, J. Wei, X. Jiang, M. Gao, X. Zheng, X. Zhang, X. Deng, C. Zhang, W. Liu, C. Cao, F. Zhang, Q. Tang, S. Ma, J. Zhao, L. Hu, Y. Shen, L. Chen, Modulating surface potential by controlling the β phase content in poly(vinylidene fluoridetrifluoroethylene) membranes enhances bone regeneration, Adv. Healthcare Mater. 7 (2018), 1701466, https://doi.org/10.1002/adhm.201701466.
[160] Y. Li, Y. Meng, Y. Bai, Y. Wang, J. Wang, B. Heng, J. Wei, X. Jiang, M. Gao, X. Zheng, X. Zhang, X. Deng, Restoring the electrical microenvironment using ferroelectric nanocomposite membranes to enhance alveolar ridge regeneration in a mini-pig preclinical model, J. Mater. Chem. B 11 (2023) 985–997, https://doi.org/10.1039/D2TB02054H.
[161] Z. Du, C. Wang, R. Zhang, X. Wang, X. Li, Applications of graphene and its derivatives in bone repair: advantages for promoting bone formation and providing real-time detection, challenges and future prospects, Int. J. Nanomed. 15 (2020) 7523–7551, https://doi.org/10.2147/IJN.S271917.
[162] J. Park, S. Park, J.E. Kim, K.J. Jang, H. Seonwoo, J.H. Chung, Enhanced osteogenic differentiation of periodontal ligament stem cells using a graphene oxide-coated poly(ε-caprolactone) scaffold, Polymers 13 (2021) 797, https://doi.org/10.3390/polym13050797.
[163] K.T. Lim, H. Seonwoo, K.S. Choi, H. Jin, K.J. Jang, J. Kim, J.W. Kim, S.Y. Kim, P. H. Choung, J.H. Chung, Pulsed-electromagnetic-field-assisted reduced graphene oxide substrates for multidifferentiation of human mesenchymal stem cells, Adv. Healthcare Mater. 5 (2016) 2069–2079, https://doi.org/10.1002/adhm.201600429.
[164] H. Yan, L. Li, Z. Wang, Y. Wang, M. Guo, X. Shi, J.M. Yeh, P. Zhang, Mussel-inspired conducting copolymer with aniline tetramer as intelligent biological adhesive for bone tissue engineering, ACS Biomater. Sci. Eng. 6 (2020) 634–646, https://doi.org/10.1021/acsbiomaterials.9b01601.
[165] S.A. Park, H. Lee, S. Kim, K. Kim, D. Jo, S. Park, Three-dimensionally printed polycaprolactone/beta-tricalcium phosphate scaffold was more effective as an rhBMP-2 carrier for new bone formation than polycaprolactone alone, J. Biomed. Mater. Res. 109 (2021) 840–848, https://doi.org/10.1002/jbm.a.37075.
[166] V. Fitzpatrick, Z. Martín-Moldes, A. Deck, R. Torres-Sanchez, A. Valat, D. Cairns, C. Li, D.L. Kaplan, Functionalized 3D-printed silk-hydroxyapatite scaffolds for enhanced bone regeneration with innervation and vascularization, Biomaterials 276 (2021), 120995, https://doi.org/10.1016/j.biomaterials.2021.120995.
[167] K. Dienel, A. Abu-Shahba, R. Kornilov, R. Björkstrand, B. van Bochove, J. Snäll, T. Wilkman, K. Mesimäki, A. Meller, J. Lindén, A. Lappalainen, J. Partanen, R. Seppänen-Kaijansinkko, J. Seppälä, B. Mannerström, Patient-specific bioimplants and reconstruction plates for mandibular defects: production workflow and in vivo large animal model study, Macromol. Biosci. 22 (2022), 2100398, https://doi.org/10.1002/mabi.202100398.
[168] C.D. Lopez, J.R. Diaz-Siso, L. Witek, J.M. Bekisz, L.F. Gil, B.N. Cronstein, R. L. Flores, A. Torroni, E.D. Rodriguez, P.G. Coelho, Dipyridamole augments three-dimensionally printed bioactive ceramic scaffolds to regenerate craniofacial bone, Plast. Reconstr. Surg. 143 (2019) 1408–1419, https://doi.org/10.1097/PRS.0000000000005531.
[169] L. Le Guéhennec, D. Van hede, E. Plougonven, G. Nolens, B. Verlée, M. De Pauw, F. Lambert, *In vitro* and *in vivo* biocompatibility of calcium-phosphate scaffolds three-dimensional printed by stereolithography for bone regeneration, J. Biomed. Mater. Res. 108 (2020) 412–425, https://doi.org/10.1002/jbm.a.36823.
[170] P. Chang, H. Luo, Z. Lin, W. Tai, C. Chang, Y. Chang, D.L. Cochran, M. Chen, Regeneration of critical-sized mandibular defect using a 3D-printed hydroxyapatite-based scaffold: an exploratory study, J. Periodontol. 92 (2021) 428–435, https://doi.org/10.1002/JPER.20-0110.
[171] A. Bhattacharjee, S. Bose, 3D printed hydroxyapatite – Zn2+ functionalized starch composite bone grafts for orthopedic and dental applications, Mater. Des. 221 (2022), 110903, https://doi.org/10.1016/j.matdes.2022.110903.
[172] M. Bartnikowski, C. Vaquette, S. Ivanovski, Workflow for highly porous resorbable custom 3D printed scaffolds using medical grade polymer for large volume alveolar bone regeneration, Clin. Oral Implants Res. 31 (2020) 431–441, https://doi.org/10.1111/clr.13579.
[173] N. Owji, A. Aldaadaa, J.R. Cha, T. Shakouri, E. García-Gareta, H.W. Kim, J. C. Knowles, Synthesis, characterization, and 3D printing of an isosorbide-based, light-curable, degradable polymer for potential application in maxillofacial reconstruction, ACS Biomater. Sci. Eng. 6 (2020) 2578–2587, https://doi.org/10.1021/acsbiomaterials.9b00884.
[174] Y. Zamani, G. Amoabediny, J. Mohammadi, H. Seddiqi, M.N. Helder, B. Zandieh-Doulabi, J. Klein-Nulend, J.H. Koolstra, 3D-printed poly(Ɛ-caprolactone) scaffold with gradient mechanical properties according to force distribution in the mandible for mandibular bone tissue engineering, J. Mech. Behav. Biomed. Mater. 104 (2020), 103638, https://doi.org/10.1016/j.jmbbm.2020.103638.
[175] R.F. Richter, T. Ahlfeld, M. Gelinsky, A. Lode, Composites consisting of calcium phosphate cements and mesoporous bioactive glasses as a 3D plottable drug delivery system, Acta Biomater. 156 (2023) 146–157, https://doi.org/10.1016/j.actbio.2022.01.034.
[176] Y.H. Chiu, I.C. Chen, C.Y. Su, H.H. Tsai, T.H. Young, H.W. Fang, Development of injectable calcium sulfate and self-setting calcium phosphate composite bone graft materials for minimally invasive surgery, Int. J. Mol. Sci. 23 (2022) 7590, https://doi.org/10.3390/ijms23147590.
[177] W. Zhang, M. Yu, Y. Cao, Z. Zhuang, K. Zhang, D. Chen, W. Liu, J. Yin, An anti-bacterial porous shape memory self-adaptive stiffened polymer for alveolar bone regeneration after tooth extraction, Bioact. Mater. 21 (2023) 450–463, https://doi.org/10.1016/j.bioactmat.2022.08.030.
[178] W. Zhang, W. Shi, S. Wu, M. Kuss, X. Jiang, J.B. Untrauer, S.P. Reid, B. Duan, 3D printed composite scaffolds with dual small molecule delivery for mandibular bone regeneration, Biofabrication 12 (2020), 035020, https://doi.org/10.1088/1758-5090/ab906e.
[179] Y. Qian, X. Zhou, H. Sun, J. Yang, Y. Chen, C. Li, H. Wang, T. Xing, F. Zhang, N. Gu, Biomimetic domain-active electrospun scaffolds facilitating bone regeneration synergistically with antibacterial efficacy for bone defects, ACS Appl. Mater. Interfaces 10 (2018) 3248–3259, https://doi.org/10.1021/acsami.7b14524.
[180] H. Liu, L. Qiu, H. Liu, F. Li, Y. Fan, L. Meng, X. Sun, C. Zhan, R. Luo, C. Wang, J. Zhang, R. Li, Effects of fiber cross-angle structures on the mechanical property of 3D printed scaffolds and performance of seeded MC3T3-e1 cells, ACS Omega 6 (2021) 33665–33675, https://doi.org/10.1021/acsomega.1c04672.
[181] Q. Zhang, J.W. Hwang, J.-H. Oh, C.H. Park, S.H. Chung, Y.-S. Lee, J.-H. Baek, H.-M. Ryoo, K.M. Woo, Effects of the fibrous topography-mediated macrophage phenotype transition on the recruitment of mesenchymal stem cells: an in vivo study, Biomaterials 149 (2017) 77–87, https://doi.org/10.1016/j.biomaterials.2017.10.007.
[182] F. Yu, R. Lian, L. Liu, T. Liu, C. Bi, K. Hong, S. Zhang, J. Ren, H. Wang, N. Ouyang, L.-J. Du, Y. Liu, L. Zhou, Y. Liu, B. Fang, Y. Li, S.-Z. Duan, L. Xia, Biomimetic hydroxyapatite nanorods promote bone regeneration via accelerating osteogenesis of BMSCs through T cell-derived IL-22, ACS Nano 16 (2022) 755–770, https://doi.org/10.1021/acsnano.1c08281.
[183] Y. He, M. Tian, X. Li, J. Hou, S. Chen, G. Yang, X. Liu, S. Zhou, A hierarchical-structured mineralized nanofiber scaffold with osteoimmunomodulatory and osteoinductive functions for enhanced alveolar bone regeneration, Adv. Healthcare Mater. 11 (2022), 2102236, https://doi.org/10.1002/adhm.202102236.
[184] S. Moeini, M.R. Mohammadi, A. Simchi, In-situ solvothermal processing of polycaprolactone/hydroxyapatite nanocomposites with enhanced mechanical and biological performance for bone tissue engineering, Bioact. Mater. 2 (2017) 146–155, https://doi.org/10.1016/j.bioactmat.2017.04.004.
[185] M.G. Gandolfi, F. Zamparini, S. Valente, G. Parchi, G. Pasquinelli, P. Taddei, C. Prati, Green hydrogels composed of sodium mannuronate/guluronate, gelatin and biointeractive calcium silicates/dicalcium phosphate dihydrate designed for oral bone defects regeneration, Nanomaterials 11 (2021) 3439, https://doi.org/10.3390/nano11123439.
[186] P. Chuysinuan, P. Nooeaid, T. Thanyacharoen, S. Techasakul, P. Pavasant, K. Kanjanamekanant, Injectable eggshell-derived hydroxyapatite-incorporated fibroin-alginate composite hydrogel for bone tissue engineering, Int. J. Biol. Macromol. 193 (2021) 799–808, https://doi.org/10.1016/j.ijbiomac.2021.10.132.
[187] M.S. Rahman, M.M. Rana, L.S. Spitzhorn, N. Akhtar, M.Z. Hasan, N. Choudhury, T. Fehm, J.T. Czernuszka, J. Adjaye, S.M. Asaduzzaman, Fabrication of biocompatible porous scaffolds based on hydroxyapatite/collagen/chitosan composite for restoration of defected maxillofacial mandible bone, Prog Biomater 8 (2019) 137–154, https://doi.org/10.1007/s40204-019-0113-x.
[188] S. Jin, R. Yang, C. Hu, S. Xiao, Y. Zuo, Y. Man, Y. Li, J. Li, Plant-derived polyphenol and LL-37 peptide-modified nanofibrous scaffolds for promotion of antibacterial activity, anti-inflammation, and type-H vascularized bone regeneration, ACS Appl. Mater. Interfaces 15 (2023) 7804–7820, https://doi.org/10.1021/acsami.2c20776.